Molecular Neurobiology (2019) 56:3005–3023
https://doi.org/10.1007/s12035-018-1272-9

AT2R Activation Prevents Microglia Pro-inflammatory Activation in a NOX-Dependent Manner: Inhibition of PKC Activation and p47^{phox} Phosphorylation by PP2A

Shahnawaz Ali Bhat[1] · Anika Sood[2] · Rakesh Shukla[1] · Kashif Hanif[1,2]

Received: 19 December 2017 / Accepted: 19 July 2018 / Published online: 3 August 2018

Abstract

Microglia-induced reactive oxygen species (ROS) production and inflammation play an imperative role in neurodegenerative diseases like Alzheimer's disease (AD) and Parkinson's disease (PD). It has been established that angiotensin II type-2 receptor (AT2R) activation is neuroprotective in central nervous system diseases like stroke and AD. However, the involvement of AT2R in NADPH oxidase (NOX)-mediated microglia activation is still elusive. Therefore, the present study investigated the role of AT2R in angiotensin II (Ang II) or Phorbol 12-myristate 13-acetate (PMA)-induced microglia activation in BV2 cells, primary microglia, p47^{phox} knockout (p47KO) microglia, and in vivo. Treatment of microglia with Ang II or PMA induced a significant ROS generation and promoted pro-inflammatory microglia in a NOX-dependent manner. In contrast, AT2R activation by CGP42112A (CGP) inhibited NOX activation, ROS production, and pro-inflammatory microglia activation, while promoting the immunoregulatory microglia. This inhibitory effect of AT2R on NOX and pro-inflammatory activation was attenuated by AT2R antagonist, PD123319. Essentially, NOX inhibition (by DPI) or scavenging cellular ROS (by NAC) or p47KO microglia were immune to Ang II- or PMA-induced pro-inflammatory microglia activation. Mechanistically, AT2R, via activation of protein phosphatase-2A (PP2A), prevented the Ang II- or PMA-induced protein kinase C (PKC) activation and phosphorylation of p47^{phox}, an effect that was reversed by the addition of PP2A inhibitor, Okadaic acid (OA). Importantly, PKC inhibitor, Rottlerin, inhibited the Ang II- or PMA-induced p47^{phox} phosphorylation and ROS generation to the similar extent as AT2R activation. In addition, AT2R activation or p47KO prevented ROS production, pro-inflammatory microglial activation, and sickness behavior in mice model of neuroinflammation. Therefore, the present findings suggested that AT2R, via PP2A-mediated inhibition of PKC, prevents the NOX activation, ROS generation, and subsequent pro-inflammatory activation of microglia.

Keywords AT2 receptor · Reactive oxygen species · NADPH oxidase · PP2A · Microglia · Neuroinflammation

Introduction

Microglia, the brain-resident macrophages, show remarkable heterogeneity [1] by displaying pro-inflammatory and the alternatively activated immunoregulatory/anti-inflammatory activation states [2–4]. The pro-inflammatory state is characterized by high levels of MHC II, CD86, IFN-γ, interleukin (IL)-1β, tumor necrosis factor-α (TNF-α), iNOS, MCP-1, and IL-12 [2–4] and increased oxidative stress [3–5]. However, immunoregulatory/anti-inflammatory state is associated with high levels of IL-4, TGF-β, IL-10, YM-1, and Arg-1 [3–5]. The pro-inflammatory activation of microglia plays the foremost role in the pathogenesis of various CNS diseases, like AD, PD, traumatic brain injury, multiple sclerosis, and stroke [1, 2, 4, 6].

Oxidative stress, particularly, microglia-generated ROS, has been well recognized in the pathogenesis of various neurodegenerative diseases like AD and PD [7–9]. Importantly, NADPH oxidase-2 (NOX-2), the main source of ROS in microglia [4, 10], is essential for pro-inflammatory activation of microglia and its inhibition promotes anti-inflammatory

Shahnawaz Ali Bhat and Anika Sood contributed equally to this work.

Electronic supplementary material The online version of this article (https://doi.org/10.1007/s12035-018-1272-9) contains supplementary material, which is available to authorized users.

✉ Kashif Hanif
k_hanif@cdri.res.in

[1] Division of Pharmacology, CSIR-Central Drug Research Institute, Lucknow, Uttar Pradesh 226031, India

[2] National Institute of Pharmaceutical Education and Research, Rae Bareli, India

microglial activation [11]. NOX-2 is a multi-subunit enzyme complex and consists of cytoplasmic ($p47^{phox}$, $p67^{phox}$, $p40^{phox}$, and Rac2) and membrane proteins ($gp91^{phox}$ and $p22^{phox}$) [11]. The phosphorylation of $p47^{phox}$ by PKC drives the activation of NOX-2 and ROS generation in microglia [12–14]. Further, increased ROS production has also been associated to mitochondrial dysfunction in microglia [6]. Therefore, it is likely that inhibition of ROS-mediated mitochondrial dysfunction can result in suppression of pro-inflammatory activation of microglia [9, 15].

Central renin-angiotensin system (RAS) is known to modulate memory functions [16, 17], and its components are expressed on both neurons and glial cells [13, 16, 18, 19]. In the brain, AT1R activation by Ang II, a potent RAS component, is associated with different physiological or pathological outcomes like integrity of BBB, sympathetic activity, stress, inflammation, behavior, and cognition [16]. In fact, treatment with AT1R blockers (ARBs) prevented CNS sympathetic activity, neuroinflammation, and cognitive decline [16]. Importantly, Ang II via AT1R induces the PKC-mediated activation of NOX-2 and ROS generation [13, 14]. Further, studies on co-culture of neurons and microglia have shown that microglial ROS via Ang II/AT1R/NOX axis resulted in neuronal death, because cultures lacking microglia were protected from Ang II-induced cell death [13, 14]. In addition, AT1R activation by Ang II has also been associated with macrophage pro-inflammatory activation [20], mitochondrial dysfunction [21] and microglia pro-inflammatory activation in brain [14]. On the other hand, Ang II also binds to AT2Rs (although its expression is far low than AT1R) and has since long been known to antagonize the actions of AT1R activation [19, 22, 23]. Importantly, the role of AT2R in anti-oxidative and anti-inflammatory activation of microglia counteracting AT1R activation has recently been reviewed [24]. However, how AT2R modulates NOX activation, ROS generation, and pro-inflammatory activation of microglia is still elusive.

We and others have demonstrated that activation of AT2R, especially during AT1R blockade, becomes important for the anti-inflammatory and neuroprotective effects of ARBs [19, 25]. Recently, the direct neuroprotective action of AT2R in stroke has been extensively demonstrated [22, 23]. Further, Iwai et al. [26] demonstrated that AT2R knockout mice following cerebral ischemia displayed larger infarcts primarily due to aggravated inflammation and increased ROS production. In addition, AT2R knockout mice exhibited impaired cognitive functions [27], and in contrast, AT2R stimulation promoted the neural differentiation and neuroprotection [28]. Similarly, the silencing of microglial AT2R exacerbated the pro-inflammatory response to LPS in vitro [29]. However, whether AT2R activation can prevent pro-inflammatory microglia activation or promote the anti-inflammatory microglia has not been investigated.

Therefore, the aim of the present study was to determine the possible role of AT2R in NOX-2 mediated microglia activation in both in vitro and in vivo conditions. Results, obtained in this study, clearly show that Ang II- or PMA-induced ROS generation resulted in pro-inflammatory activation of microglia and mitochondrial dysfunction in a NOX-dependent manner. Most importantly, we, for the first time to our knowledge, demonstrated that AT2R via PP2A-mediated inhibition of PKC prevented the NOX activation, ROS generation, and subsequent pro-inflammatory activation of microglia.

Materials and Methods

Reagents and Antibodies

MitoSOX red (Cat. No. M36008), antibiotic/antimycotic solution (15240062), fetal bovine serum (10438026), and trypsin (25200056) were purchased from Invitrogen (Carlsbad, CA, USA). CGP (AT2R agonist; C160), *N*-acetylcysteine (NAC; A7250), Dulbecco's modified Eagle's medium-F12 (DMEM-F12; D8900), diphenyliodonium (DPI; 43,088), 2′,7′-ichlorofluorescin diacetate (DCF-DA; 35,845), 3,3′,5,5′-tetramethylbenzidine (TMB; T2885), 5,5′,6,6′-tetrachloro-1,1′,3,3′-tetraethylbenzimidazolecarbocyanine Iodide (JC-1; 420,200), and other chemicals otherwise revealed were from Sigma (St. Louis, MO, USA). Primary antibodies to YM-1 (ab192029), Arg-1 (ab60176), iNOS (ab15323), CD86 (ab112490), MHC II (ab180779), phospho-S9-GSK-3 (ab131097), phospho-Y216-GSK-3 (ab75745), total-GSK-3 (ab32391), AT1R (ab18801), and AT2R (ab19134) were from Abcam (USA), p-T638/641-PKCα/β (9375) and p-T505-PKCδ (9374) from Cell Science and Technology (USA), p-S345-$p47^{phox}$ (SAB4504721), p-Y307-PP2A (SAB4503975), and β-actin (A5441) from Sigma (USA), $gp91^{phox}$ (sc-130,543), $p22^{phox}$ (sc-271,968), $p47^{phox}$ (sc-17,844), NRF-2 (sc-722), and histone H3 (sc-8654) from Santa Cruz (USA), and Alexa Fluor 594 and Alexa Fluor 488 IgG conjugate (Invitrogen) and secondary HRP-conjugated antibodies were purchased from Santa Cruz Biotechnology (USA). ELISA kits for IL-10 (900-M53) and TNF-α (900-T54) were purchased from Peprotech (USA).

Cell Culture

Murine microglial cell line (BV2) and neuronal cell line Neuro2A were obtained from the National Centre for Cell Sciences, Pune, India, and maintained in the tissue culture facility of CSIR-Central Drug Research Institute (CSIR-CDRI), Lucknow, India. BV2 cells were cultured in DMEM/F12 medium supplemented with 10% heat-inactivated fetal

bovine serum at 37 °C in a humidified atmosphere of 5% CO_2. For experiments, BV2 cells were seeded into 6/12-well tissue culture plates at a density of 1–4 × 10^5cells/well. After 24 h, cells were washed with PBS, to remove the serum, and incubated in serum-free media for an additional 24 h, prior to any treatment. The involvement of AT2R in Ang II- (1–1000 nM) or PMA-induced (10 ng/mL) [30] M1 polarization was studied by employing CGP (AT2R agonist) at different concentrations (0.5 to 5 μM) or PD123319 (AT2R antagonist) (1 μM) [13, 19]. The role of ROS was elucidated by using ROS scavenger, NAC (5 mM) [14] or NOX-2 inhibitor, DPI (1 μM) [31]. The role of mitochondrial dysfunction and GSK-3β in microglia polarization was elucidated by employing mito-Tempo (200 μM) [32] and SB216763 (10 μM) [33], respectively. The involvement of PKC and PP2A was revealed by using their respective inhibitors: Rottlerin (5 μM) [34] and Okadaic acid (500 nM) [12].

Primary Microglia Culture

The primary microglia were isolated from mixed glial cultures as described previously [35, 36]. Briefly, cerebral hemispheres, taken from 2- to 3-day-old wild-type (WT) or $p47^{phox}$ knockout (p47KO) mice pups, were mechanically chopped and single-cell suspension was obtained. The mixed glial cell suspension from two brains were plated in a 75-cm^2 vented cell culture flask with DMEM/F12 medium supplemented with 10% FBS and 1% (*v*/*v*) penicillin-streptomycin solution and grown in a humidified 5% CO_2 incubator at 37 °C. On days 14 to 21 in vitro, microglia were detached using an orbital shaker (180 rpm, 5 h, 37 °C) and centrifuged (150×*g*, 15 min), and microglia number and viability were assessed by trypan blue exclusion using hemocytometer. Depending on the experiment, microglia were plated in either 96-well cell culture plates or 6-well cell culture plates in DMEM/F12 supplemented with 10% FBS and 1% (*v*/*v*) penicillin-streptomycin and placed in a humidified 5% CO_2 incubator at 37 °C. The purity of microglia was around 95–99% as confirmed by Iba-1 immunostaining (Supplementary Fig. 1a). The primary or p47KO microglia were treated as above.

Cell Viability Assay

Cell viability was determined by the tetrazolium salt 3-[4,5-dimethylthiazol-2-yl]-2,5- diphenyltetrazolium bromide (MTT; Sigma, St. Louis, MO, USA) assay as described previously [19]. The optical density was measured spectrophotometrically at 530 nM, and results are expressed as a percentage of surviving cells compared with the control. We do not find any cellular toxicity of various treatments in microglia (Supplementary Fig. 1b, c).

ROS Production

To measure level of ROS like H_2O_2 and O_2^- in BV2 and primary microglia, DCF-DA and DHE dyes were respectively used by employing flow cytometry and fluorescent microscopy. Cells grown in 12- or 6-well plates (1–2 × 10^5 cells/well, respectively) were treated as specified and incubated for 30 min with DCF-DA (5 μM)/DHE (5 μM) at the end of the treatment. Then, the cells were washed with phosphate-buffered saline (PBS) twice and DCF/DHE-positive microglia, 10,000 counts per condition, were quantified using the FACS Calibur (BD) with the Cell Quest software [19]. For imaging experiments, the DCF/DHE-positive BV2 cells after the specified treatments, were first washed with PBS, and then imaged using a fluorescent microscope (Lieca, Germany). The mean fluorescence intensity of DCF/DHE positive cells was calculated using ImageJ software (NIH), and presented as percentage change from control.

MitoSOX red (5 μM) was used to examine the mitochondrial ROS (mtROS) level by using flow cytometry. After the specified treatments, cells were incubated with MitoSOX red, 30 min before the finishing point of the treatment. Finally, the cells were washed and data was acquired on a FACS Calibur (BD) and quantified with the Cell Quest software.

Determination of Cellular ATP Levels

The ATP level in microglia was estimated using ATP assay kit (Abcam, USA) by following the manufacturer's instructions. In brief, following the specified treatment, the microglia were lysed in a reaction buffer and centrifugation was done at 15,000×*g* for 2 min to remove the debris. To 50 μL of resulting supernatant, 50 μL of ATP reaction mix was added in a 96-well plate. After 30 min incubation, absorbance was measured at 570 nm in ELISA plate reader (BIOTEK) [17]. The concentration of ATP was calculated from ATP standard curve and expressed in nanomoles per milligram of protein.

Mitochondrial Membrane Potential (ψm)

The difference in the mitochondrial membrane potential (Δψm) was determined by flow cytometry using JC-1 dye as described previously [37]. During physiological conditions, the dye gets accumulated in the mitochondrial matrix and forms J aggregates, owing to the mitochondrial membrane potential, with a characteristic absorption and emission spectra that can be determined by flow cytometry. In brief, BV2 microglia after different stimulations were incubated with JC-1 dye (2.5 μM) in culture medium for 30 min at 37 °C. The cells were washed with PBS twice, and mitochondrial membrane potential (Δψm) was assessed using FACS Calibur (FACS Calibur, Becton Dickinson, NJ, USA) and analyzed by Cell Quest program (Becton Dickinson, NJ, USA).

Extracellular Flux Assay

The effects of AT2R activation on cellular respiratory functions in BV2 microglia were measured using a Seahorse XFP flux analyzer (Seahorse Bioscience, Billerica, MA, USA) as described previously [37]. Briefly, BV2 cells were grown onto Seahorse assay plates (10,000 cells/well) and were treated with Ang II in the presence or absence of AT2R agonist, CGP. The medium was changed to XF assay medium (HCO_3-free modified DMEM; Seahorse Bioscience) supplemented with 4 mM L-glutamine and 1 mM pyruvate, pH 7.4, and cells were maintained at 37 °C in a non-CO_2 incubator for 2 h. After baseline measurements of oxygen consumption rate (OCR), a mitochondrial respiration test was carried out by chronological addition of 0.5 μM oligomycin, 1 μM FCCP, and 1 μM rotenone/antimycin A. The parameters determined were basal respiration, maximal respiratory capacity, spare respiratory capacity, proton leak, and non-mitochondrial respiration. In each case, the results were expressed as OCR in picomoles per minute. An archetypal OCR tracing from mitochondrial respiratory function as measured by Seahorse XFP flux analyzer (Seahorse Bioscience, Billerica, MA, USA) and derivation of each parameter is shown in Supplementary Fig. 4a. After the completion of the experiment, the cells were lysed for measurement of protein content in order to normalize the respiration data.

Immunocytochemistry and Confocal Microscopy

Immunocytochemical analysis was done in microglia as described previously [19, 36]. In brief, cells grown on coverslips were fixed with ice-cold 4% paraformaldehyde in PBS for 10 min. Cells were blocked using 1% BSA + 0.3% (*v*/*v*) Triton X-100 + 0.3 M glycine (1% BSA) in PBS for 45 min at room temperature. The cells were incubated with primary antibodies, goat Iba-1 (1:200), rabbit anti-AT1R (1:100), anti-AT2R (1:100), goat anti-gp91^{phox}, and mouse anti-p47^{phox} diluted in 1% BSA at 4 °C overnight. Cells were washed with PBS, followed by 2 h incubation with the secondary antibody, Alexa Fluor 488 and 594 respective IgG conjugates (Invitrogen, USA) at room temperature. Coverslips were mounted with Prolong Gold antifade mounting medium (Invitrogen, USA). Images were acquired with a confocal microscope (BX61WI, Olympus, Japan) and were processed by using Image J software (NIH).

Cytokine Levels

The cytokine level in the culture supernatant of BV2 microglia or primary microglia were estimated by ELISA using specific ELISA kits (Peprotech, USA), according to the manufacturer's instructions as described previously [19, 36].

Protein Extraction and Immunoblotting

Proteins extracted from microglia were processed for western blotting as described previously [19, 36]. Nuclear and cytosolic fractions were prepared using hypotonic and hypertonic lysis buffer as previously described [19, 36]. In brief, an equal amount of protein was separated on 10% SDS-PAGE and transferred to PVDF membrane. Membranes were blocked with blocking buffer (5% BSA, 10 mM Tris, pH 7.5, 100 mM NaCl, and 0.1% Tween-20) for 2 h. After blocking, the membranes were incubated with respective primary antibodies—rabbit anti-AT1R (1:1000), anti-AT2R (1:500), anti-Arg-1 (1:1000), anti-YM1 (1:2000), anti-iNOS (1:500), anti-p22^{phox} (1:500), anti-histone H3 (1:1000), anti-p-S-9GSK-3β (1:1000), mouse anti-MHC II (1:1000), anti-p-Y-216-GSK-3β (1:1000), anti-p47^{phox} (1:300), anti-β-actin (1:10,000), and goat anti-GSK-3β (1:1000) and anti-gp91^{phox} (1:500) overnight at 4 °C. After washing, membranes were incubated with respective HRP-conjugated secondary antibodies (1:5000) for 2 h at room temperature. The protein bands were visualized by chemiluminescence reagents (Millipore, USA). The band intensity was measured using spot densitometry analysis by myImageAnalysis™ software (Thermo Scientific) [19, 36].

RNA Preparation and RT-PCR

Quantitative gene expression analysis was performed by using SYBR Green technology as described previously [38]. Briefly, the total RNA was extracted from different groups using TRIZOL (Sigma, USA) isolation procedure and cDNA was synthesized using RevertAid™ H Minus first-strand cDNA synthesis kit following the manufacturer's protocol (Invitrogen, USA). mRNA expression of key genes associated with the phenotype change during microglia polarization was quantified using specific primers (Supplementary Table 1). Real-time RT-PCR was carried out in QuantStudio 12K Flex Real-Time PCR System (Applied Biosciences Indianapolis, USA). Relative mRNA expression was calculated by using comparative cycle threshold ($2^{-\Delta\Delta}$ Ct) method using GAPDH as an internal standard [38], and the relative amount of mRNA was presented in the form of fold change over control.

PP2A Activity

PP2A activity in cell lysate was measured by using p-nitrophenyl phosphate (pNPP) as substrate as described previously [19, 39]. In brief, after various stimulations, the cell lysate (20 μL) was incubated with 5 mM pNPP for 15 min followed by the addition of Malachite green solution (50 μL), and the color was allowed to develop for 30 min at room temperature. Absorbance at 620 nM was measured, and

phosphate release was quantified by comparison with inorganic phosphate standards as described previously [19].

Analysis of Apoptotic Cell Death

The conditioned media from microglia after various treatments as indicated for 24 h was collected and centrifuged to remove cell debris as described previously [19, 36]. In brief, Neuro2A cells in a 12-well format (2×10^5 cells/well) were treated with the conditioned media from microglia for 24 h and were stained with Annexin V-FITC and PI according to the manufacturer's instructions (BD Biosciences) followed by flow cytometric analysis. Data was acquired by using FACS Calibur (BD Biosciences) collecting 10,000 events. The differentiation of early apoptotic, late apoptotic, necroptotic, and viable cells was made according to their phenotype: Annexin V^+/PI^- were considered early apoptotic, Annexin V^-/PI^+, necroptotic, Annexin V^+/PI^+ late apoptotic, and Annexin V^-/PI^- viable cells.

Assessment of Effect of AT2R Activation on the Expression of M1 and M2 Markers in a Mouse Model of Neuroinflammation

Eight-week-old male WT and p47KO mice both of C57BL/6 background (22–25 g) were used in the present study. We carried out all the experiments in the male mice. Knockout [B69 (Cg)-Ncf1^{m1j}/J], and their littermate controls were procured from Jackson Labs, USA. Mice were housed in IVC cages (Tecniplast, Italy) and provided food and water ad libitum. All the experiments were approved by the Institutional Animal Ethics Committee (IAEC) of CSIR-CDRI and Committee for the Purpose of Control and Supervision of Experiments on Animals (CPCSEA), India. For LPS-induced neuroinflammation, dose of LPS (250 μg/kg, i.p.) was selected from the studies of Lee et al. [40]. For the role of AT2R, CGP42112 at a dose of 1 mg/kg [41] was administered in mice intraperitonially 5 days prior to the LPS administration. After acclimatization, the mice were randomly distributed into five groups. Each group had a minimum of four to six mice: control (group I, $n = 6$), LPS (250 μg/kg; group II, $n = 6$), LPS + CGP (1 mg/kg; group III, $n = 6$), p47KO (group IV, $n = 4$), and LPS + p47KO (group IV, $n = 4$).

To assess LPS-induced sickness behavior (characterized by the decrease in the locomotor activity), [42], open-field test was performed [42] by Optovarimax (OptoM-3, Columbus Instruments, USA) [43]. Mice were individually placed in locomotor boxes (42.5 × 42.5 × 35 cm) to evaluate horizontal/ambulatory activity and rearing activity, respectively [43]. Locomotor boxes consist of transparent Plexiglas with a grid of fully automated infrared emitters and detectors to measure the activity by the number of infrared beam crossed by the animal [44]. As indexes of locomotor activity, ambulatory counts (number of individual horizontal movements recorded when the mice walked on all four feet) and vertical counts (rearing counts registered when the body of mice inclined vertically with hind paws on the floor and forepaws on the wall of the activity cage) were evaluated [44]. The locomotor activity was monitored over a period of 10 min [44]. The open-field arena was swabbed every time with 10% alcohol to avoid the odor interference of previous animal.

At the end of the behavioral assessment, the mice were killed by transcardiac perfusion with saline under diethyl ether anesthesia. Brains were collected and cortical region was separated on an ice-cold plate and immediately stored at − 80 °C for western, qPCR, or ELISA analysis of M1- or M2-like expression, as described earlier.

Statistical Analysis

Statistical analysis was performed with Prism software version 5.0 (Graph Pad Software, San Diego, CA, USA). Results are expressed as mean ± SEM. Data in Fig. 1c, d was analyzed by repeated measure one-way analysis of variance (ANOVA) followed by Tukey's multiple comparison test. Rest, all the statistical significance was evaluated by one-way analysis of variance (ANOVA) followed by Tukey's multiple comparison test, unless otherwise stated. A value of $p < 0.05$ was considered to be statistically significant.

Results

AT2R Activation Prevents Ang II-Induced RAS Over-activation in Microglia

First, we confirmed the presence of angiotensin receptors, i.e., AT1R and AT2R in BV2 microglia by confocal microscopy (Supplementary Fig. 2a) and qPCR (Supplementary Fig. 2b). Stimulation of microglia with Ang II-induced RAS over-activation as evident from increased protein expression of AT1R and decreased AT2R expression in microglia (Supplementary Fig. 2d). However, activation of AT2R by CGP in a concentration dependent manner, prevented the Ang II-induced AT1R expression, while increased the AT2R expression in microglia (Supplementary Fig. 2c, d). The increase in the expression of AT2R following CGP treatment was reversed by the pre-treatment with AT2R antagonist, PD123319 (Supplementary Fig. 2c), confirming the specificity of CGP for AT2R.

AT2R Activation Prevents Ang II-Induced ROS Generation in Microglia in a NOX-Dependent Manner

Treatment of BV2 microglia with Ang II (1 to 1000 nM) in a concentration-dependent manner induced an increase

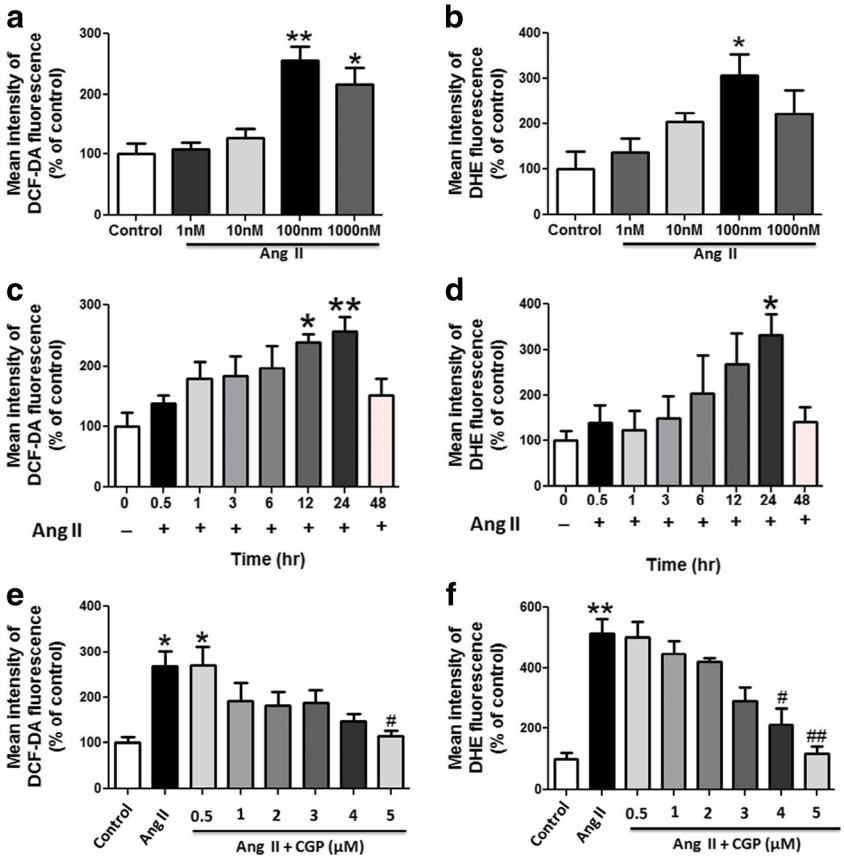

Fig. 1 AT2R activation prevented Ang II-induced ROS production in microglia. ROS (H_2O_2 and superoxide generation) was determined by flow cytometric analysis of DCF- and DHE-positive BV2 microglia. Ang II in a **a** concentration- (1–1000 nM) and **b** time-dependent (0–48 h) manner-induced ROS generation in BV2 microglia. Highest ROS generation was observed at 100 nM concentration (**a**) after 24 h (**b**). However, AT2R activation by CGP, an AT2R agonist, in a concentration-dependent (0.5–5 μM) manner prevented Ang II-induced ROS generation in BV2 microglia. **e**, **f** Maximum ROS suppression was observed at 5 μM concentration of CGP. Data represent mean ± SEM of at least three independent experiments, each with two to three internal replicates ($n \geq 3$); $^{*}p < 0.05$ and $^{**}p < 0.01$ versus control group; $^{\#}p < 0.05$ and $^{\#\#}p < 0.01$ versus Ang II group (one-way ANOVA followed by post hoc Tukey's test)

in ROS levels, with a significant increase at 100 and 1000 nM, as assessed by flow cytometric analysis and fluorescent microscopic observation of DCF^+ and DHE^+ cells (Fig. 1a, b; Supplementary Fig. 3a). After 24 h interval and at 100 nM concentration, Ang II induced a maximum increase in ROS levels in BV2 microglia (Fig. 1a–d; Supplementary Fig. 3a, b, $p < 0.05$–0.01); therefore, further experiments were carried out only at this time point and concentration of Ang II (100 nM). Further, AT2R activation by CGP (0.5 to 5 μM), in a concentration-dependent manner deceased the Ang II-induced ROS generation, as evident by the decrease in the fluorescent intensity of DCF^+ and DHE^+ in BV2 microglia (Fig. 1e, f; Supplementary Fig. 3b). However, the significant and maximum inhibition of ROS production was achieved only at 5 μM; therefore, this concentration was selected for further experiments (Fig. 1e, f). These observations established that AT2R activation inhibits Ang II-induced ROS production in microglia.

Since NOX-2 is the major source of ROS in microglia [4], we therefore assessed the involvement of NOX in ROS production following Ang II treatment of BV2 microglia. Ang II induced NOX activation, as apparent from the increased $gp91^{phox}$, $p22^{phox}$, and $p47^{phox}$ expressions in the membrane fraction (Fig. 2a, b), resulting in ROS production in microglia (Fig. 2c, d). On the contrary, AT2R activation by CGP significantly reversed the Ang II-induced NOX activation (as evident from decreased expression of $gp91^{phox}$, $p22^{phox}$, and $p47^{phox}$) and ROS production in microglia (Fig. 2a–d). More relevantly, AT2R-mediated NOX suppression, as indicated by $p47^{phox}$ translocation to plasma membrane and mitigation of ROS (Fig. 2a–d) was remarkably blunted by PD123319, a well-established AT2R inhibitor (Fig. 2a–d). Further, as expected, inhibition of NOX by DPI or scavenging cellular ROS by NAC prevented Ang II-induced NOX activation and ROS production in microglia (Fig. 2a–d), confirming the role of NOX-2 in Ang II-mediated ROS production.

To further validate that AT2R prevented NOX-mediated ROS generation, the BV2 microglia were stimulated with the PMA in the presence or absence of CGP (Fig. 2e). As expected, PMA induced significant NOX activation (increased $gp91^{phox}$ and translocation of p47 to membrane) (Fig. 2e) and ROS generation in the microglia (Supplementary Fig. 3c, d). On the contrary, AT2R activation by CGP prevented the PMA-induced NOX activation (Fig. 2e) and ROS generation in microglia (Supplementary Fig. 3c, d). However, CGP alone had no effect on either basal ROS levels or $p47^{phox}$ and $p22^{phox}$ expression in microglia cells (Supplementary Fig. 4a–c). These results firmly validate that AT2R, by suppression of NOX activation, prevents ROS generation in microglia.

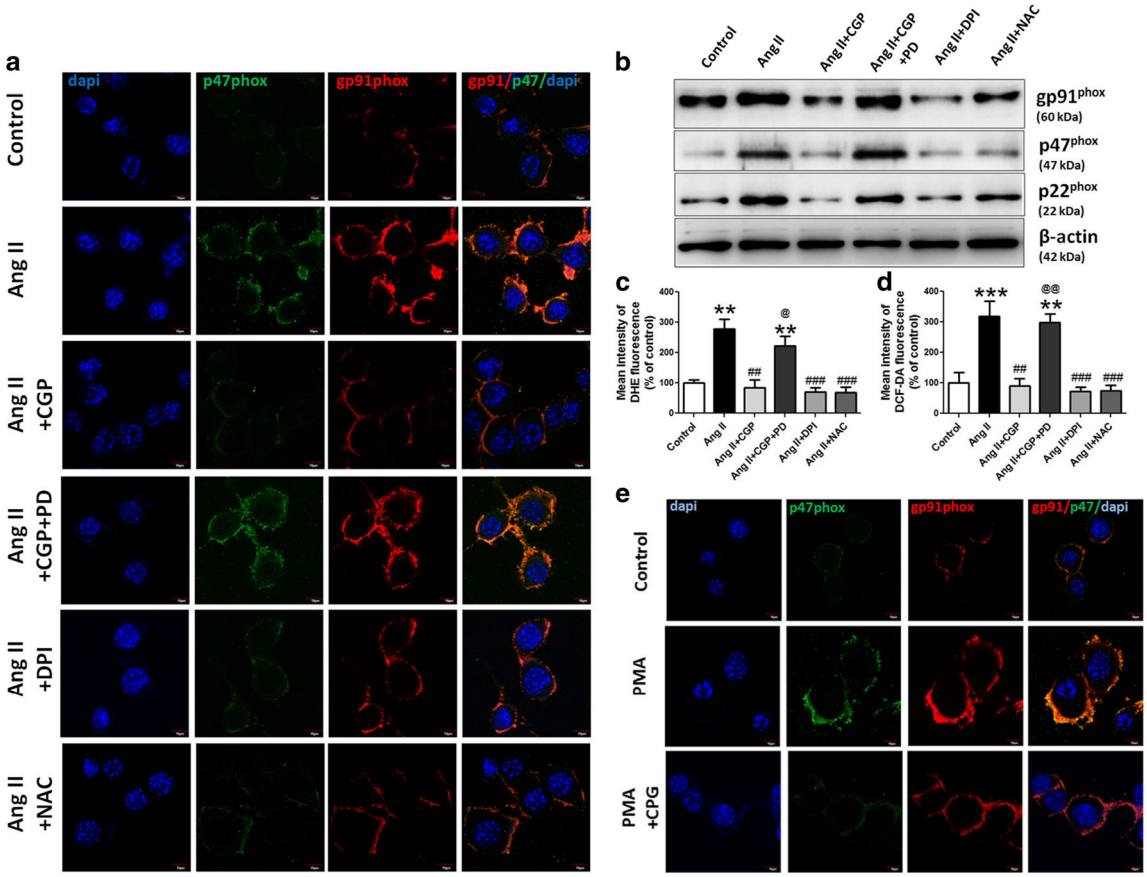

Fig. 2 AT2R activation inhibited NOX-2 activation and ROS generation in Ang II- and PMA-stimulated BV2 microglia. **a** Representative confocal images showing overlay of $p47^{phox}$ and $gp91^{phox}$ (NOX-2 subunits) in different treatment groups. **b** Representative immunoblots of $gp91^{phox}$, $p47^{phox}$, and $p22^{phox}$ expression, normalized by β-actin expression. **c** ROS generation represented as DCF and DHE fluorescence percentage change in BV2 microglia pre-treated with AT2R agonist (CGP), CGP and PD (AT2R antagonist), NADPH oxidase inhibitor (DPI), and ROS scavenger treatment (NAC) 30 min prior to Ang II stimulation (100 nM). Ang II, angiotensin II (100 nM); Ang II + CGP, Ang II + CGP (5 μM); Ang II + CGP + PD, Ang II + CGP + PD123319 (1 μM); Ang II + DPI, Ang II + diphenyliodinium (1 μM); Ang II + NAC, Ang II + *N*-acetylcysteine (5 mM). **d** Representative confocal microscopy images showing overlay of $p47^{phox}$ and $gp91^{phox}$ in AT2R pre-treated and PMA-stimulated BV2 microglia. PMA, phorbol 12-myristate 13-acetate (10 ng/mL); PMA + CGP, PMA + CGP (5 μM). Data represent mean ± SEM of at least three independent experiments, each with two to three internal replicates ($n \geq 3$); $^{**}p < 0.01$ and $^{***}p < 0.001$ versus control group; $^{\#\#}p < 0.01$ and $^{\#\#\#}p < 0.01$ versus Ang II group; $^{@}p < 0.05$ and $^{@@}p < 0.01$ versus Ang + CGP group (one-way ANOVA followed by post hoc Tukey's test)

AT2R Activation Prevents ROS-Mediated Pro-inflammatory Microglial Activation

Microglia activation state is generally characterized by the expression of signature genes/proteins associated with the pro-inflammatory- or anti-inflammatory-like phenotype. To confirm the role of NOX in mediating Ang II-induced microglial activation, we stimulated the BV2 cells with Ang II. The treatment of BV2 microglia with Ang II induced the mRNA or protein expression of pro-inflammatory markers MHC II, iNOS, MCP-1, IL-1β, IL-6, and TNF-α (Fig. 3a–e, i, and k) and decreased gene or protein expression of immunomodulatory markers Arg-1, YM-1, IL-10, and TGF-β (Fig. 3f–j). In contrast, treatment with NAC (ROS scavenger) and inhibition of the NOX-2 by DPI prevented the Ang II-induced microglial pro-inflammatory activation, validating the involvement of ROS in shaping the microglial pro-inflammatory activation (Fig. 3a–k). These results demonstrated that Ang II, through activation of NOX-2, promotes ROS generation and pro-inflammatory microglia activation.

We next confirmed the role of AT2R in microglial activation. Ang II via AT1R-induced microglial pro-inflammatory activation as evident from increased expression of iNOS and MHC II expression and decreased expression of Arg-1 in microglial cells (Supplementary Fig. 4d–g). AT1R blockade by Candesartan or AT2R activation by CGP prevented the Ang II-induced upregulation of iNOS and MHC II expression and increased expression of Arg-1 (Supplementary Fig. 4d–g). To verify whether AT2R activation after AT1R blockade by Candesartan inhibited the pro-inflammatory microglial activation, we hypothesized that blockade of AT2R would reverse the

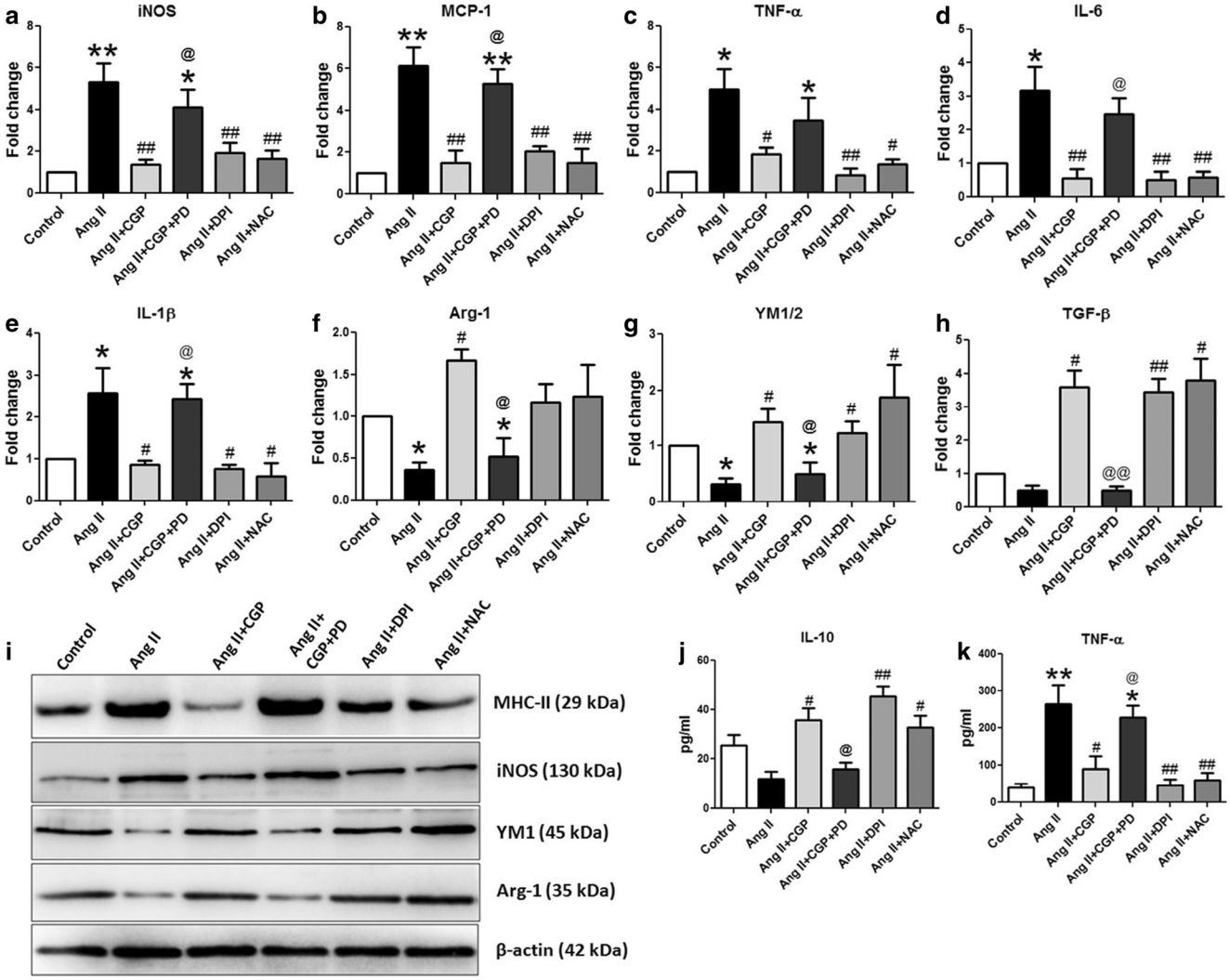

Fig. 3 AT2R activation prevented microglia M1-like polarization, while it promoted M2-like polarization in Ang II-stimulated BV2 microglia. **a**–**e** qPCR measurement of mRNA expression of pro-inflammatory signature genes (iNOS, MCP-1, TNF-α, IL-6, and IL-1β) in BV2 cells pre-treated with CGP, CGP and PD, DPI, and NAC following Ang II stimulation. **f**, **g** qPCR analysis of immunoregulatory signature genes (Arg-1, YM-1, and TGF-β) in BV2 microglia. **i** Representative immunoblots of pro-inflammatory (MHC I I , iNOS) and immunoregulatory (YM1, Arg-1) protein expression that were normalized by β-actin expression. ELISA estimation of protein concentrations of **j** immunoregulatory mediator IL-10 and **k** pro-inflammatory mediator TNF-α in culture media of BV2 microglia at 24 h after various treatments. AT2R activation by CGP suppressed Ang II-induced M1-like marker expression and promoted M2-like marker expression in BV2 microglia, which were markedly inhibited by PD (AT2R antagonist). Ang II, angiotensin II (100 nM); Ang II + CGP, Ang II + CGP (5 μM); Ang II+CGP + PD, Ang II + CGP + PD123319 (1 μM); Ang II + DPI, Ang II + diphenyliodinium (1 μM); Ang II + NAC, Ang II + *N*-acetylcysteine (5 mM). Data represent mean ± SEM of at least three independent experiments, each with two to three internal replicates ($n \geq 3$); $^{*}p < 0.05$ and $^{**}p < 0.01$ versus control group; $^{\#}p < 0.05$ and $^{\#\#}p < 0.01$ versus Ang II group; $^{@}p < 0.05$ and $^{@@}p < 0.01$ versus Ang + CGP group (one-way ANOVA followed by post hoc Tukey's test)

protective effect of Candesartan in microglia. Importantly, the suppression of the protective effect of AT1R blockade by Candesartan on Ang II-induced pro-inflammatory microglial activation was blunted by the concomitant inhibition of AT2R with PD123319 in microglia as evident from the increased expression of pro-inflammatory iNOS and MHC II and decreased expression of anti-inflammatory Arg-1 in microglia (Supplementary Fig. 4d–g). However, CGP per se had no effect on the expression of either pro-inflammatory iNOS and MHC II or anti-inflammatory Arg-1 in microglia (Supplementary Fig. 4d–g). These results advocate the role of AT2R in microglial activation.

Notably, we earlier observed that AT2R, by suppression of NOX-2 activation, prevented ROS generation in microglia. Therefore, we studied the role of AT2R in Ang II-induced pro-inflammatory microglial activation. AT2R activation by CGP prevented the ROS-mediated pro-inflammatory activation of microglia, apparent from the decreased mRNA or protein expression of pro-inflammatory markers like MHC II, iNOS, MCP-1,

IL-1β, IL-6, and TNF-α (Fig. 3a–e, i, and k) and increased mRNA or protein expression of anti-inflammatory markers Arg-1, YM-1, IL-10 and TGF-β (Fig. 3f–j). In contrast, PD123319, an AT2R antagonist, blunted the AT2R-mediated anti-inflammatory activation of BV2 microglia (Fig. 3a–k). These results confirmed that the beneficial effects of CGP are mediated by AT2R activation.

We further validated the role of AT2R suppressed ROS generation in microglia activation by treating the BV2 cells with PMA in the presence or absence of AT2R agonist, CGP. Treatment of microglia with PMA induced the mRNA or protein expression of pro-inflammatory markers MHC II, iNOS, MCP-1, IL-1β, IL-6, and TNF-α (Fig. 4a–e, i, and k) and decreased mRNA or protein expression of anti-inflammatory markers Arg-1, YM-1, IL-10, and TGF-β (Fig. 4f–j). In contrast, AT2R activation by CGP prevented the PMA-induced pro-inflammatory activation of microglia as evident from the suppression of pro-inflammatory markers and increase in anti-inflammatory markers (Fig. 4a–j) in BV2 microglia. These observations strongly suggest that AT2R, by decreasing ROS production, prevents Ang II-induced pro-inflammatory microglial activation.

AT2R Activation Inhibited ROS-Mediated Mitochondrial Dysfunction and Associated Pro-inflammatory Microglial Activation

Since ROS impairs mitochondrial functions, known to play a key role in microglial activation, therefore, we examined the

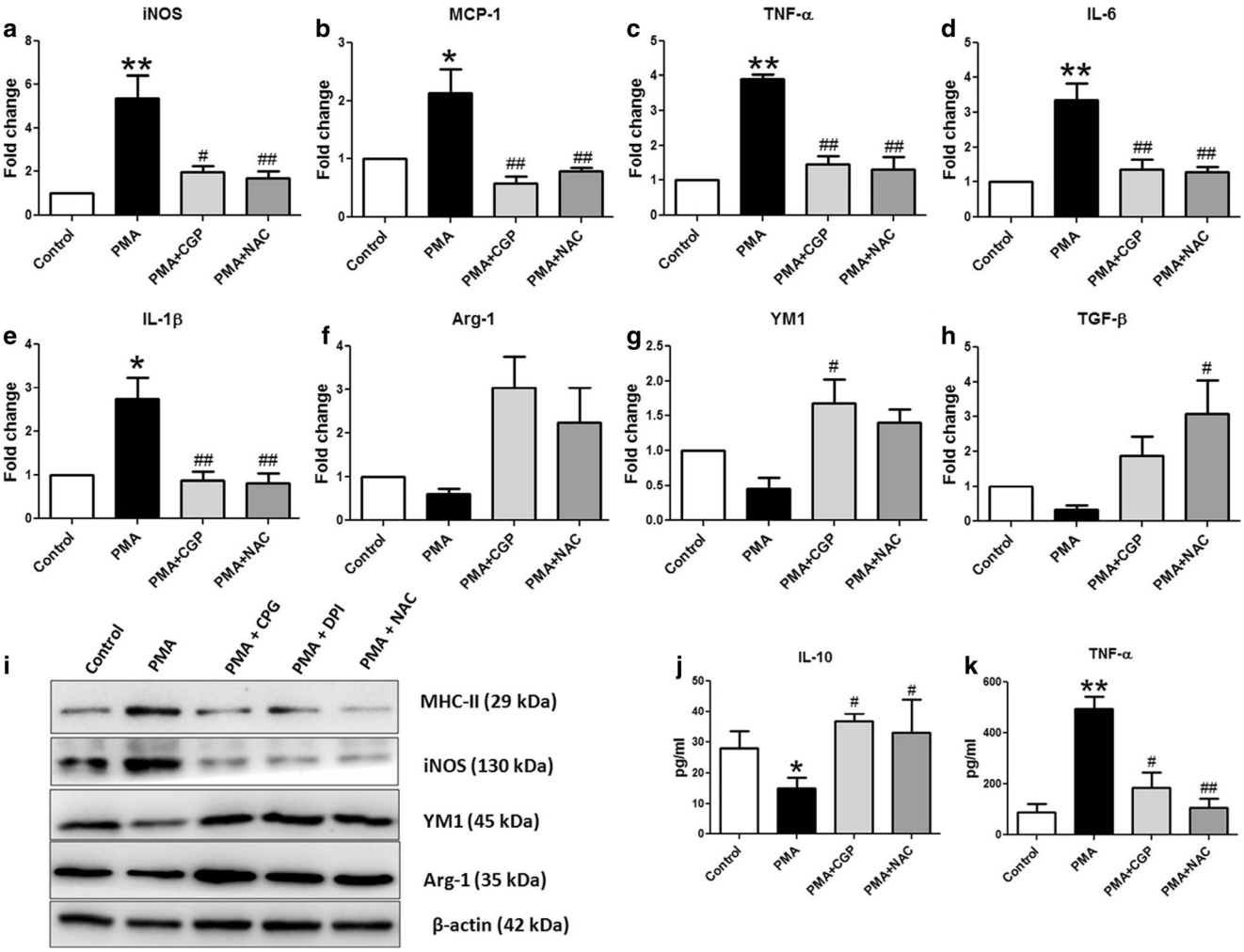

Fig. 4 AT2R activation suppressed pro-inflammatory microglia M1-like polarization, while it promoted immunoregulatory M2-like phenotype in PMA-stimulated BV2 microglia. **a**–**e** qPCR measurement of mRNA expression of M1 genes (iNOS, MCP-1, TNF-α, IL-6, and IL-1β) in BV2 cells pre-treated with CGP and NAC following PMA stimulation. **f**, **g** qPCR analysis of M2 genes (Arg-1, YM-1, and TGF-β) in BV2 microglia. **i** Representative immunoblots of M1 (MHC II, iNOS) and M2 (YM1, Arg-1) protein expression that were normalized by β-actin expression. ELISA estimation of protein concentrations of **j** M2 mediator IL-10 and **k** M1 mediator TNF-α in culture media of BV2 microglia at 24 h after various treatments. PMA, phorbol 12-myristate 13-acetate; PMA + CGP, PMA + CGP (5 μM); PMA + NAC, PMA + *N*-acetylcysteine (5 mM). Data represent mean ± SEM of at least three independent experiments, each with two to three internal replicates ($n \geq 3$); $^{*}p < 0.05$ and $^{**}p < 0.01$ versus control group; $^{\#}p < 0.05$ and $^{\#\#}p < 0.01$ versus PMA group (one-way ANOVA followed by post hoc Tukey's test)

mitochondrial functions following Ang II treatment in BV2 microglia. Treatment of BV2 microglia with Ang II impaired mitochondrial functions as apparent from the loss of mitochondrial membrane potential (increased depolarized mitochondria) (Fig. 5a, b), increase in the mitochondrial ROS (increased MitoSOX Red fluorescence) (Fig. 5c) and decrease in the cellular ATP level (Fig. 5d). To determine the effects of AT2R activation on energy metabolism in BV2 microglia, cells were treated with Ang II in the presence of AT2R agonist, CGP for 24 h, followed by measurement of mitochondrial respiration. Treatment with Ang II or CGP had no significant effect on basal respiration or non-mitochondrial respiration of the microglia (Supplementary Fig. 5b, c). However, Ang II impaired maximal respiration and spare reserve capacity of BV2 microglia (Fig. 5e–g). In contrast, AT2R activation by CGP prevented mitochondrial dysfunction (evident from increase in the ATP level, high mitochondrial membrane potential, suppression of mitochondrial ROS, and improved

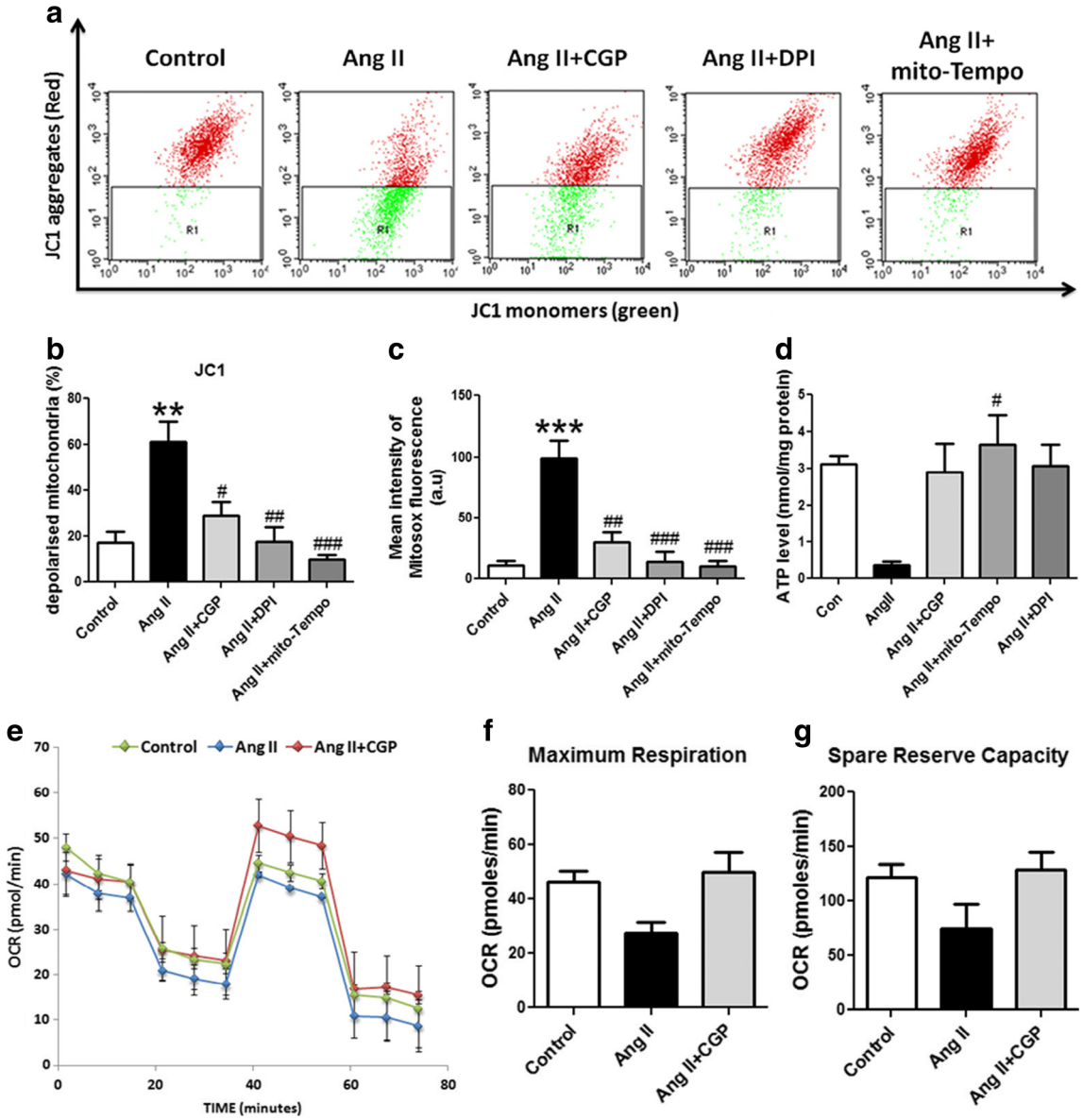

Fig. 5 AT2R activation prevented Ang II-induced mitochondrial dysfunction in BV2 microglia. **a** Flow cytometric analysis of JC-1 aggregates following different stimulations in BV2 microglia. Cells after different stimulations were incubated with JC-1 dye for 30 min at 37 °C. Bar graphs representing **b** percent depolarized mitochondria, **c** MitoSOX fluorescence intensity, and **d** ATP level following different stimulations in BV2 microglia. **e**–**g** AT2R activation improved mitochondrial respiration in BV2 microglia as determined by the real-time analysis of OCR. Ang, angiotensin II (100 nM); Ang II + CGP, Ang II + CGP (5 μM); A + DPI, Ang II + diphenyliodinium (1 μM); A + mito-Tempo, Ang II + Mito-Tempo (200 μM). Data represent mean ± SEM of at least three independent experiments, each with two to three internal replicates ($n \geq 3$); $^{***}p < 0.001$ versus control group; $^{\#\#}p < 0.01$ and $^{\#\#\#}p < 0.001$ versus Ang II group (one-way ANOVA followed by post hoc Tukey's test)

mitochondrial respiration) (Fig. 5a–g) following Ang II treatment. NOX inhibition by DPI inhibited the Ang II-induced mitochondrial dysfunction in BV2 microglia (Fig. 5a–d), confirming the role of NOX-2-derived ROS in the mitochondrial dysfunction. These observations provide the evidence that AT2R activation improves mitochondrial functions.

Involvement of mitochondrial dysfunction in microglial pro-inflammatory activation became apparent when treatment with Mito-Tempo (which suppresses mitochondrial ROS) reversed the Ang II-induced mitochondrial dysfunction and pro-inflammatory microglia activation, as evident from the significant decrease in mRNA or protein expression of pro-inflammatory markers MHC II, iNOS, MCP-1, IFN-γ, IL-1β, IL-6, and TNF-α (Fig. 6a–e, i, and k) and increase in mRNA or protein expression of anti-inflammatory markers Arg-1, YM-1, IL-10, and TGF-b (Fig. 6f–j). Equally, AT2R activation by CGP improved mitochondrial functions and prevented pro-inflammatory activation of microglia following Ang II treatment (Fig. 6a–j). These data strongly suggest that ROS-mediated mitochondrial dysfunction by NOX-2 activation is central to microglia pro-inflammatory activation and AT2R, via NOX-2 inhibition, improves mitochondrial functions and, thereby, prevents pro-inflammatory microglia activation.

AT2R Activation Prevented Oxidative Stress-Mediated GSK-3 Activation, NRF2 Degradation, and Pro-inflammatory Microglial Activation

Increased oxidative stress is associated with the activation of GSK-3β, a well-known inducer of pro-inflammatory

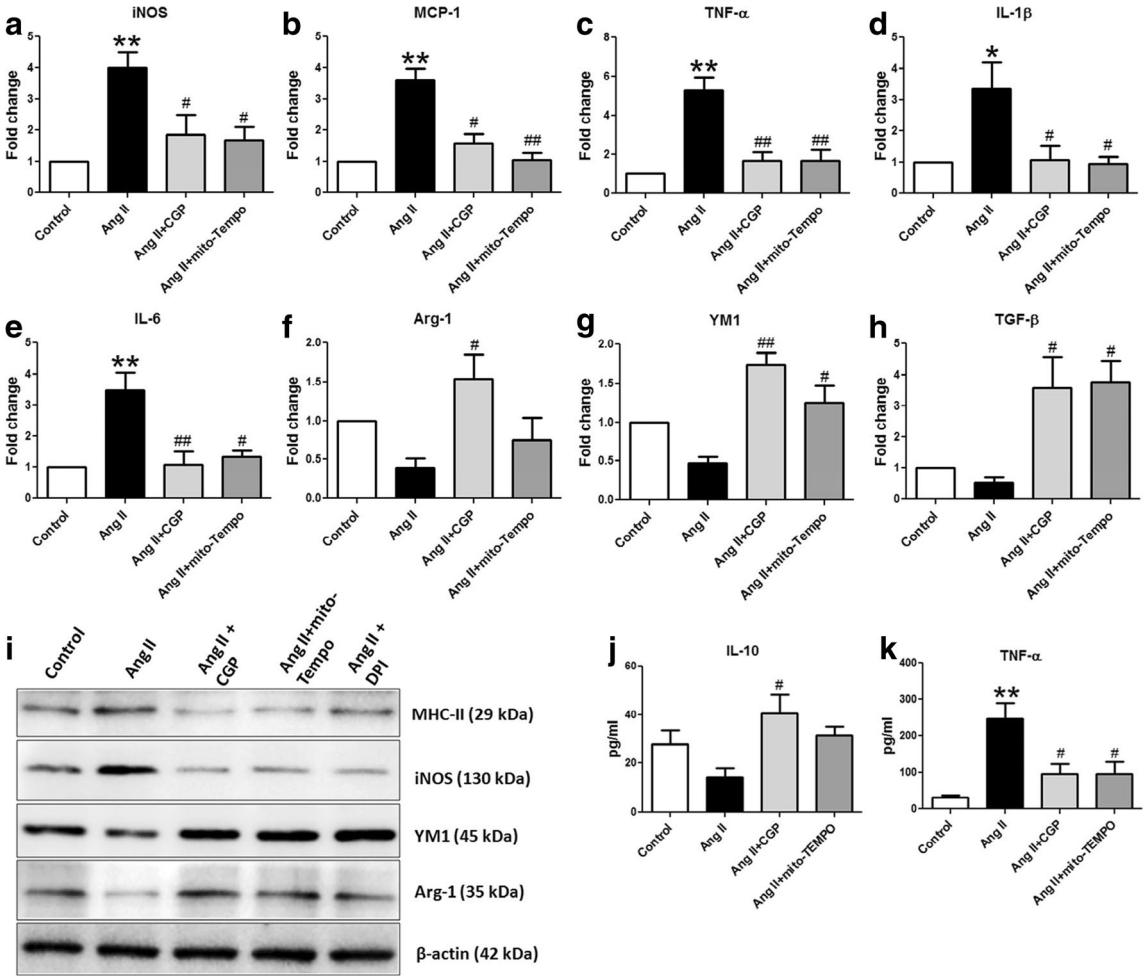

Fig. 6 AT2R activation promoted the immunoregulatory microglia by improving mitochondrial functions in BV2 microglia. **a**–**e** qPCR measurement of mRNA expression of M1-like markers (iNOS, MCP-1, TNF-α, IL-6, and IL-1β) in BV2 cells pre-treated with CGP, mito-Tempo, and DPI following Ang II stimulation. **f**, **g** qPCR analysis of M2-like markers (Arg-1, YM-1, and TGF-β) in BV2 microglia. **i** Representative immunoblots of M1 (MHC II, iNOS) and M2 (YM1, Arg-1) protein expression after various treatment regimens. The release of inflammatory cytokines **j** M2 mediator IL-10 and **k** M1 mediator TNF-α in culture media of BV2 microglia at 24 h after various treatments was estimated by ELISA. Ang, angiotensin II (100 nM); Ang II + CGP, Ang II + CGP (5 μM); A + DPI, Ang II + diphenyliodinium (1 μM); A + mito-Tempo, Ang II + Mito-Tempo (200 μM).). Data represent mean ± SEM of at least three independent experiments, each with two to three internal replicates ($n \geq 3$); $^{*}p < 0.05$ and $^{**}p < 0.01$ versus control group; $^{\#}p < 0.05$ and $^{\#\#}p < 0.01$ versus Ang II group (one-way ANOVA followed by post hoc Tukey's test)

microglial activation [45], which in turn degrades the NRF2 which is vital for the antioxidant protection of microglia [45]. Therefore, we investigated the involvement of ROS in activation of GSK-3β and NRF2 nuclear expression in the BV2 microglia cells. Treatment with Ang II induced GSK-3β activation as evident from the increased phosphorylation of Y-216 residue (Supplementary Fig. 6a) and decreased phosphorylation of S-9 residue of GSK-3β (Supplementary Fig. 6a), with a significant decrease in the nuclear expression of NRF2 (Supplementary Fig. 6b), anti-oxidant GSH and HO-1 expression (Supplementary Fig. 6c, d), and pro-inflammatory activation of microglia (Supplementary Figs. 6e and 7a–d). However, GSK-3β inhibition by SB216763 prevented GSK-3β activation (Supplementary Fig. 6a), reduction in the nuclear expression of NRF2 (Supplementary Fig. 6b), GSH, and HO-1 expression (Supplementary Fig. 6c, d) and associated pro-inflammatory microglia activation (decreased pro-inflammatory markers like iNOS, MHC II, TNF, IL-6; Supplementary Figs. 6e and 7a–d). These results underlined the involvement of GSK-3β in microglial pro-inflammatory activation.

The involvement of ROS in the GSK-3β activation in BV2 microglia was established by treatment with antioxidant NAC. NAC prevented the Ang II-induced GSK-3β activation (Supplementary Fig. 6a), increased the nuclear NRF2 expression (Supplementary Fig. 6b), and prevented pro-inflammatory microglia activation (Supplementary Fig. 7a–i) in BV2 microglia. Likewise, AT2R activation by CGP prevented GSK-3β activation (significant decrease in phosphor-Y-216/phospho-S-9 GSK-3β ratio) (Supplementary Fig. 6a) and increased the nuclear NRF2 expression (Supplementary Fig. 6b) with subsequent increase in the GSH and HO-1 expression (Supplementary Fig. 6c, d). Further, AT2R activation by CGP prevented pro-inflammatory microglia activation (decrease in pro-inflammatory markers MHC II, iNOS, CD86, IFN-γ, IL-1β, IL-6, and TNF-α) and increase in anti-inflammatory markers (Arg-1, YM-1, IL-10, and TGF) in microglia following Ang II treatment (Supplementary Figs. 6e and 7a–i). These results demonstrated AT2R as a potent inhibitor of oxidative stress-induced GSK-3β activation and NRF2 degradation and associated pro-inflammatory M1-like microglia.

AT2R Prevented NOX-2 Activation and Pro-inflammatory Polarization of Microglia byPP2A-Mediated Inhibition of PKC

Since, Ang II via AT1R and PMA by direct activation of PKC induces NOX-2 activation (by phosphorylation of $p47^{phox}$) and ROS generation [12–14], therefore, we investigated the effects of AT2R on PKC activation (PKC δ and α/β the major PKC isoforms that are responsible for PKC-mediated microglial activation) [34] in BV2 microglia. Ang II or PMA treatment induced the PKC activation as evident from increased of major PKC isoforms, p-PKCα/β and p-PKCδ in microglia. However, we observed a robust activation of p-PKCδ isoform during Ang II or PMA treatment in microglia cells (Fig. 7a). Further, activation of PKC was associated with the increased phosphorylation of $p47^{phox}$ and ROS production in these cells (Fig. 7a). In order to examine whether PKC-δ was involved in Ang II- or PMA-induced $p47^{phox}$ phosphorylation, NOX activation, and ROS generation, BV2 microglia were treated with Rottlerin, a specific inhibitor of PKC-δ, stimulated with Ang II or PMA. AT2R activation by CGP or PKC-δ inhibitor, Rottlerin prevented Ang II- or PMA-induced $p47^{phox}$ phosphorylation, NOX activation, and ROS generation (Fig. 7a–e). These data clearly suggested that AT2R mediated inhibition of PKC, prevented the NOX activation and ROS generation in microglia.

Further, PKC activation is known to inhibit the PP2A, a phosphatase, responsible for the dephosphorylation and inactivation of PKC, during NOX activation [12]. Importantly, we and others have reported that AT2R induces the PP2A activation in different cell types including BV2 microglia [19, 25]. Therefore, we hypothesized that AT2R might prevent NOX-2 activation and pro-inflammatory polarization of microglia via PP2A-mediated inhibition of PKC and dephosphorylation of $p47^{phox}$. We investigated the effect of PP2A inhibition on AT2R-mediated suppression of PKC, NOX-2, ROS generation and pro-inflammatory induction in BV2 microglia. Importantly, AT2R activation by CGP or PKC inhibition by Rottlerin prevented the Ang II- or PMA-induced inhibition the activity of PP2A (Fig. 7b); however, OA abolished the CGP- or Rottlerin-mediated increase in PP2A activity (Fig. 7b). Further, AT2R activation by CGP induced PP2A activation (decreased p-Y307-PP2A expression) and prevented the NOX-2 activation (suppression of p-S345-$p47^{phox}$ expression), ROS generation (decreased DCF^+ and DHE^+ cells), and subsequent pro-inflammatory activation of microglia (decreased iNOS while increasing the Arg-1 expression), which were abolished by the PP2A inhibitor, OA in BV2 cells (Fig. 7a–f). These results indicate that AT2R via PP2A activation prevents NOX activation, ROS generation, and pro-inflammatory activation in microglia.

AT2R Activation or p47KO Promoted M2-Like Polarization of Primary Microglia

To validate the data obtained from the BV2 cell line, we further investigated whether the AT2R activation by CGP prevented pro-inflammatory activation in primary microglia via inhibition of NOX-2 mediated ROS generation and associated mitochondrial dysfunction. CGP treatment not only prevented the Ang II-suppressed AT2R expression but also increased it in primary microglia (Fig. 8a). In the presence of Ang II, AT2R activation significantly prevented ROS

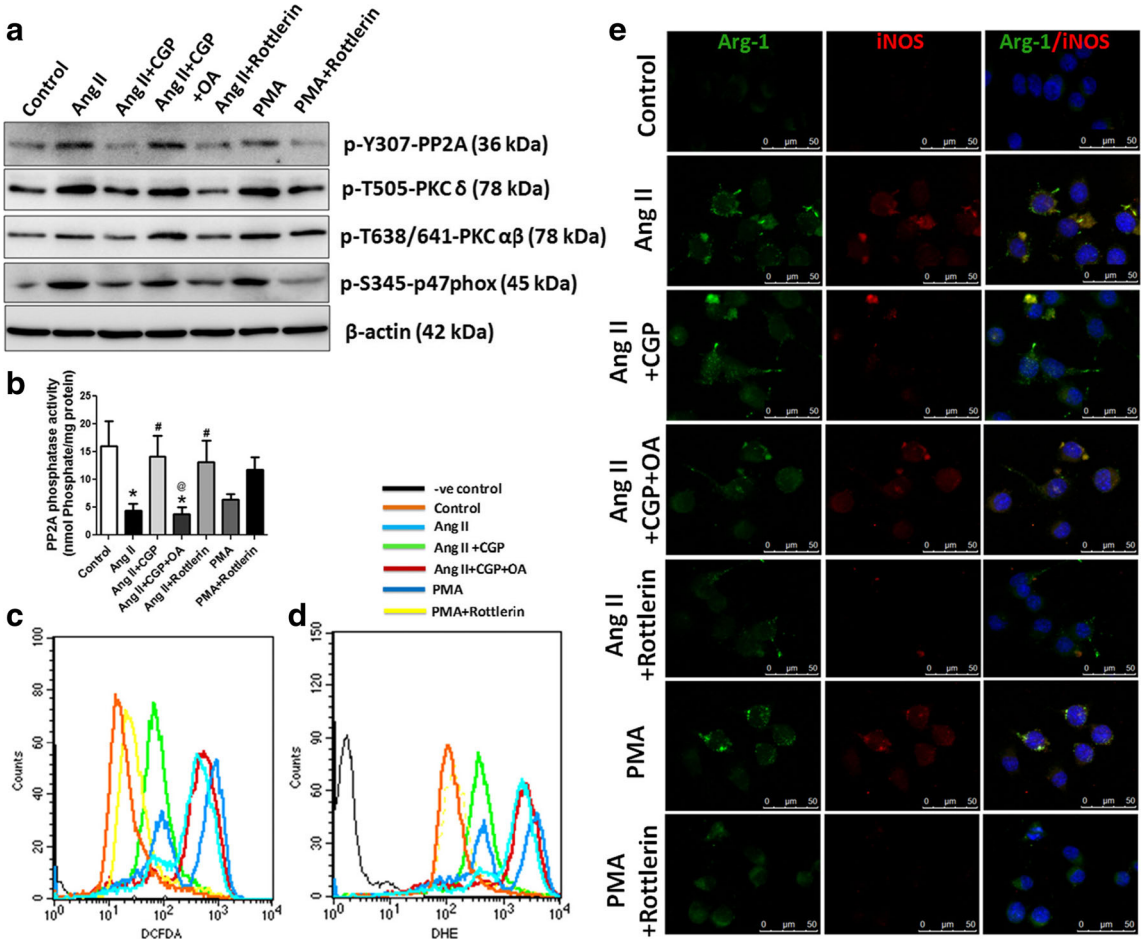

Fig. 7 AT2R prevented NOX-2 activation and pro-inflammatory polarization of microglia by PP2A-mediated inhibition of PKC and dephosphorylation of p47^{phox}. **a** Representative immunoblots of p-Y307-PP2A, p-T505-PKCδ, p-T638/641-PKCαβ, and p-S345-p47^{phox} protein expression after various treatment regimens in Ang II or PMA-stimulated BV2 microglia. AT2R via PP2A prevented Ang II- or PMA-induced PKC activation and p-47^{phox} phosphorylation in BV2 microglia, which was reversed by the AT2R inhibitor, PD123319 (PD). **b** PP2A activity. **c**, **d** Overlay of DHE and DCF fluorescence in microglia pre-treated with AT2R agonist (CGP), CGP along with OA (PP2A inhibitor), and Rottlerin, 30 min prior to Ang II or PMA stimulation as analyzed by flow cytometrically. **e** Representative co-immunostained images of pro-inflammatory iNOS and immunoregulatory Arg-1 protein expression in BV2 microglia after various treatments. Scale bar, 50 μM. Data represent mean ± SEM of at least three independent experiments ($n \geq 3$). Data represent mean ± SEM of at least three independent experiments, each with two to three internal replicates ($n \geq 3$); $^{*}p < 0.05$ versus control group; $^{\#}p < 0.05$, $^{\#\#}p < 0.01$, and $^{\#\#\#}p < 0.001$ versus Ang II group; $^{@}p < 0.05$ versus Ang II + CGP group (one-way ANOVA followed by post hoc Tukey's test)

generation (Fig. 8b, c) and mitochondrial dysfunction in primary microglia (Fig. 8d–f). Moreover, in primary microglia, CGP or NAC or SB or mito-Tempo remarkably attenuated Ang II-induced expression of pro-inflammatory markers (iNOS, TNF-α, IL-6, and MHC II) (Fig. 8g, h, k, m, and n) but enhanced immunoregulatory markers (Arg-1, YM1, and IL-10) (Fig. 8j and l–n). Both effects of AT2R activation by CGP, that is, attenuation of ROS generation and pro-inflammatory markers or enhancement of immunoregulatory markers in Ang II-stimulated primary microglia, were abolished by the AT2R inhibitor PD123319 (Fig. 8b–m).

To confirm the involvement of NOX in mediating pro-inflammatory activation of microglia, studies on p47KO microglia in the presence or absence of Ang II or PMA were conducted. Stimulation of p47KO microglia with Ang II or PMA failed to induce ROS generation (Fig. 9a, b) and pro-inflammatory activation of microglia (Fig. 9c–f). Taken together, these results strongly indicate that AT2R mediated immunoregulatory activation of primary microglia is dependent on suppression of NOX-mediated ROS generation.

AT2R Activation Prevented Neuronal Cell Death Induced by Conditioned Media from Pro-inflammatory-Activated Microglia

Since pro-inflammatory-activated microglia is categorized as neurotoxic, and immunoregulatory as neuroprotective, therefore neurons (Neuro-2A cells) were exposed to conditioned media (CM), from pro-inflammatory-activated microglia stimulated with Ang II in the absence or presence of CGP or

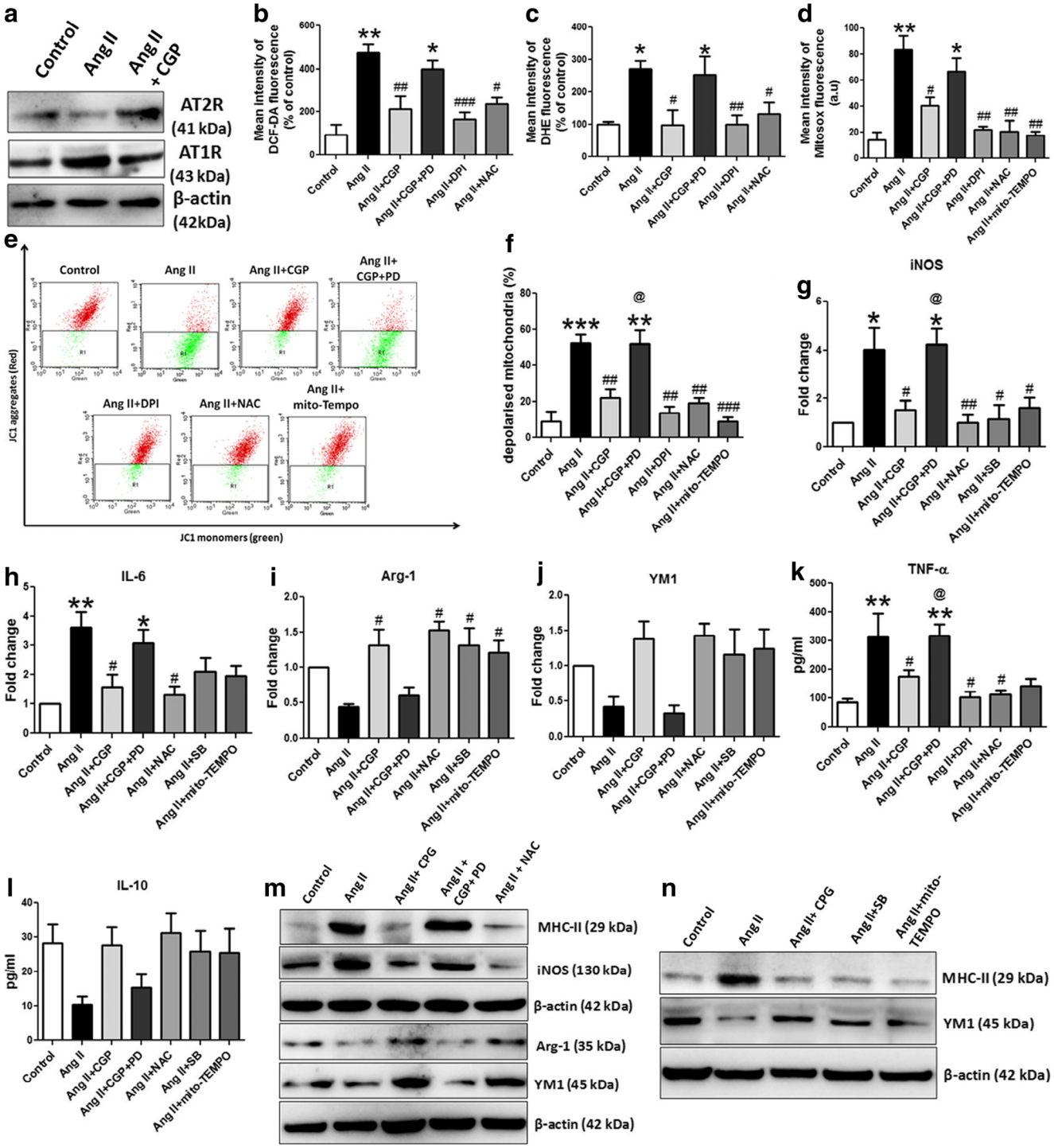

Fig. 8 AT2R activation inhibited ROS production and mitochondrial dysfunction and promoted M2 polarization in primary microglia. **a** CGP treatment increased AT2R expression in primary microglia. ROS generation represented as **b** DCF and **c** DHE fluorescence percentage change in primary microglia pre-treated with AT2R agonist (CGP), CGP and PD (AT2R antagonist), NADPH oxidase inhibitor (DPI), and ROS scavenger treatment (NAC) 30 min prior to Ang II stimulation (100 nM) as analyzed by flow cytometrically. Flow cytometric analysis of **d** MitoSOX and **e** JC-1 aggregates following different stimulations in primary microglia. **f** Quantification of (**e**). **g**, **j** qPCR measurement of mRNA expression of M1 (iNOS, IL-6) and M2 (Arg-1 and YM-1) marker genes in primary microglia pre-treated with CGP or NAC or SB or mito-Tempo following Ang II stimulation. The release of **k** M1 mediator TNF-α and **l** M2 mediator IL-10 in culture media of primary microglia at 24 h after various treatments was estimated by ELISA. **m**, **n** Representative immunoblots of M1 (MHC II, iNOS) and M2 (YM1, Arg-1) protein expression after various treatment regimens in primary microglia. AT2R suppressed Ang II-induced expression of M1 markers and promoted expression of M2 markers in primary microglia was reversed by the AT2R inhibitor, PD. Data represent mean ± SEM of at least three independent experiments, each with two to three internal replicates ($n \geq 3$); $^{*}p < 0.05$ and $^{**}p < 0.01$ versus control group; $^{\#}p < 0.05$, $^{\#\#}p < 0.01$, and $^{\#\#\#}p < 0.001$ versus Ang II group (one-way ANOVA followed by post hoc Tukey's test)

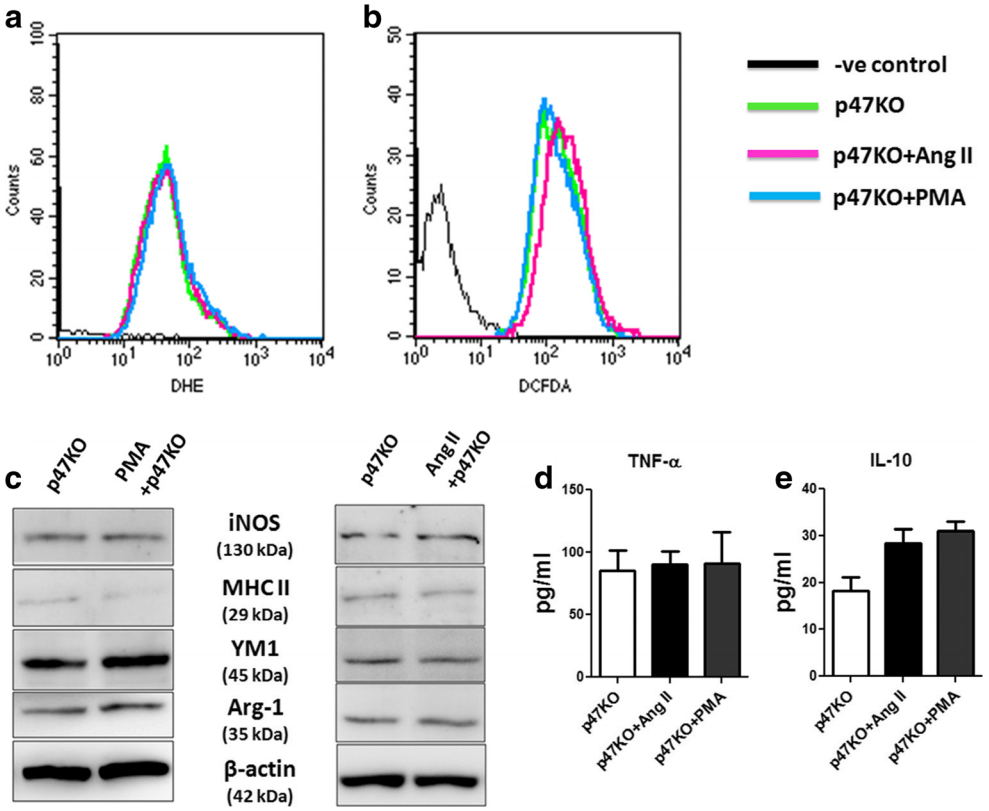

Fig. 9 p47KO microglia were immune to Ang II/PMA-induced ROS generation and M1 polarization. ROS generation in **a** superoxide and **b** H_2O_2 was determined by flow cytometric analysis of DHE- and DCF-positive p47KO microglia stimulated with Ang II or PMA. **c**, **d** Representative immunoblots of protein expression of M1 markers (MHC II, iNOS) and M2 markers (YM1, Arg-1) in p47KO microglia stimulated with Ang II or PMA. β-Actin was used as an internal control. ELISA estimation of protein concentrations of **e** pro-inflammatory mediator TNF-α and **f** immunomodulatory mediator IL-10 in culture media of p47KO microglia at 24 h after various treatments. Ang II, angiotensin II; PMA, phorbol 12-myristate 13-acetate; p47KO, $p47^{phox-/-}$. Data represent mean ± SEM of at least three independent experiments, each with two to three internal replicates ($n \geq 3$; one-way ANOVA followed by post hoc Tukey's test)

NAC, for a period of 24 h. CM from un-stimulated cells served as control. CM from Ang II-stimulated microglia induced the apoptosis of Neuro2A cells as evident from increased Annexin V-PI-positive cells (Supplementary Fig. 8). On the contrary, CM from microglia pre-treated with CGP (AT2R agonist) prevented the apoptosis (decrease in the number of Annexin V-PI-positive cells) in Neuro2A cells that was reversed by AT2R antagonist, PD123319 (Supplementary Fig. 8). Likewise, CM from microglia pre-treated with antioxidant, NAC or NOX inhibitor, DPI mitigated the apoptotic cell death in Neuro2A cells. These results functionally demonstrate that AT2R activation prevents the polarization of microglia to neurotoxic one.

AT2R Activation or p47KO Prevented LPS-Induced Sickness Behavior and M1-Like Polarization in Mice Model of Neuroinflammation

To investigate whether our in vitro findings could be translated in vivo, microglial polarization markers were assessed in the cortex in LPS-induced neuroinflammation model (a widely accepted model of microglial activation and polarization) [42]. Since LPS induces the sickness behavior, therefore we also evaluated the sickness behavior in the open-field test. We found that LPS-induced sickness behavior in mice as evident from reduced locomotion (Fig. 10a, b), which was prevented by AT2R activation by CGP (1 mg/kg Fig. 10a, b). Importantly, p47KO mice were immune to the LPS-induced sickness behavior (Fig. 10a, b) and interestingly, were found to be more active than wild-type mice (Fig. 10a, b).

Further, LPS-induced ROS generation (increased DHE^+ cells) (Fig. 10i) and pro-inflammatory activation of microglia as evidenced by the significant increase in iNOS, MCP-1, IL-1β, TNF-α, and MHC II and reduced immunoregulatory markers YM1, Arg-1, and IL-10 in the cerebral cortex (Fig. 10c–j). Conversely, AT2R activation by CGP (1 mg/kg) or p47KO significantly prevented the LPS-induced ROS generation and pro-inflammatory activation of microglia (decrease in iNOS, MCP-1, IL-1β, TNF-α, and MHC II), while promoting the immunoregulatory activation of microglia (increase in YM1, Arg-1, and IL-10) (Fig. 10c–j). Taken together, these results strongly indicate that AT2R activation or

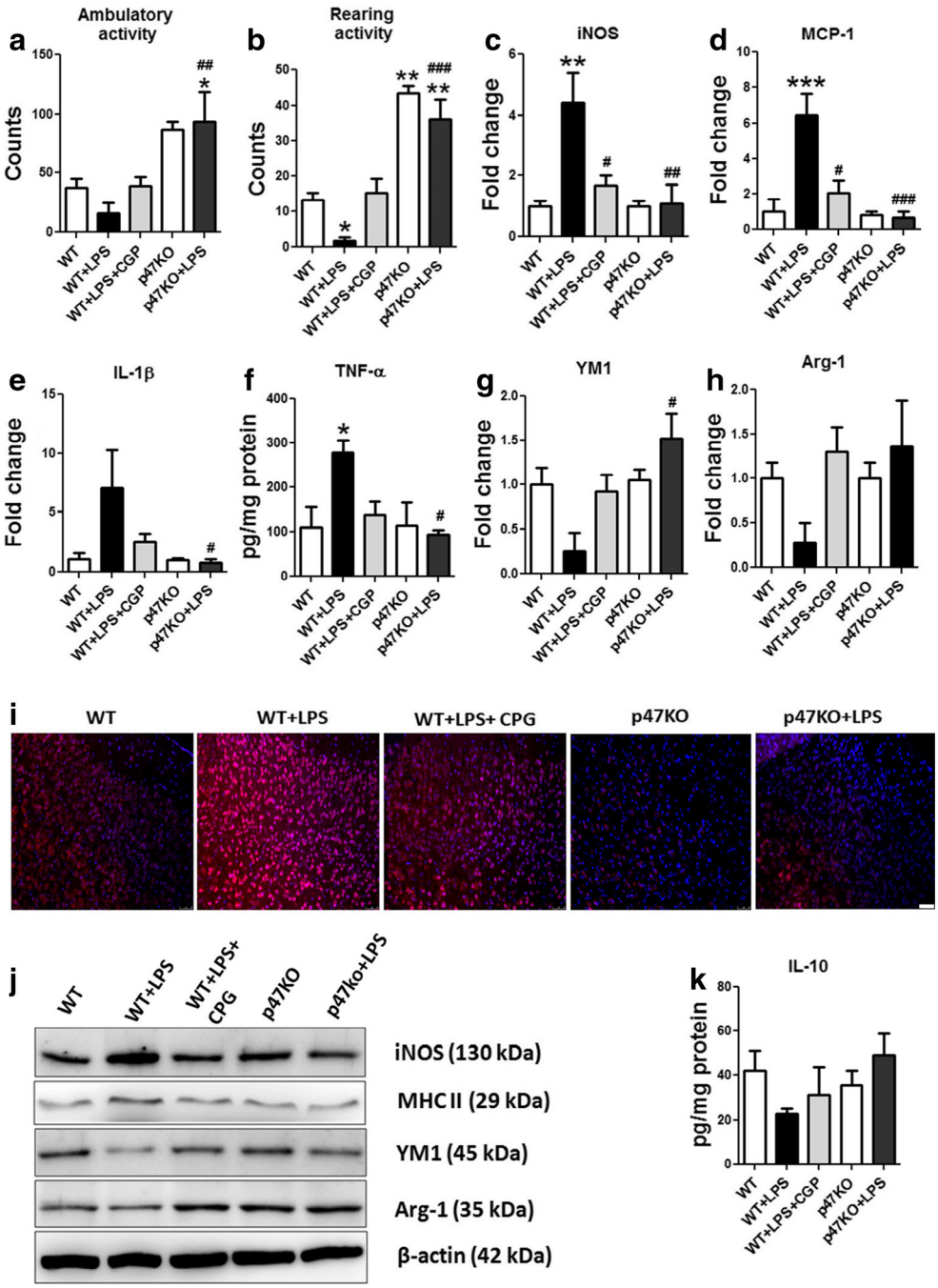

Fig. 10 AT2R activation or p47KO suppressed M1 polarization and sickness behavior in an in vivo microglia-mediated neuroinflammation model. CGP treatment or p47KO ameliorated LPS-induced sickness. **a** Ambulatory activity and **b** rearing activity (presented as counts generated by the interruption of adjacent photobeams) in an open-field test ($n = 4–6$). **c**–**e** CGP (1 mg/kg) treatment or p47KO attenuated the mRNA expression of M1 markers (iNOS, MCP-1, and IL-1β) and **f** reduced the TNF-α level in the cortex of LPS-challenged mice. **g**, **h** CGP (1 mg/kg) treatment or p47KO enhanced the mRNA expression of M2 markers YM1 and Arg-1 and **i** increased the anti-inflammatory IL-10 levels in the cortex of LPS-injected mice. **j** Representative immunoblots of M1 (MHC II, iNOS) and M2 (YM1, Arg-1) protein expression in the cortex of CGP (1 mg/kg) treated or p47KO mice at 24 h after LPS-injection. Data represent mean ± SEM ($n = 4–6$); $^{*}p < 0.05$, $^{**}p < 0.01$, and $^{***}p < 0.001$, compared with control mice; $^{\#}p < 0.05$, $^{\#\#}p < 0.01$, and $^{\#\#\#}p < 0.001$, compared with LPS-injected mice (one-way ANOVA followed by post hoc Tukey's test)

NOX inhibition attenuates ROS generation, pro-inflammatory activation of microglia, and sickness behavior in vivo.

Discussion

Microglia-induced inflammation plays an imperative role in several CNS disorders [1, 2, 4, 6]. First advocated for macrophages, the notion of alternative activation states, pro-inflammatory M1-like and immunoregulatory M2-like activation, was also extended for microglia [1, 11]. The immunoregulatory M2-like microglia are categorized as anti-inflammatory and neuroprotective, while pro-inflammatory M1-like microglia are classified as neurotoxic [4, 15]. The increased ROS production (oxidative stress), especially from microglia, has been demonstrated to contribute in the development of several neurodegenerative diseases like AD and PD [9, 46]. On the other hand, AT2R, one of the components of RAS, has been established to play a role in neuroprotection; however, the involvement of AT2R in NOX-mediated pro-inflammatory microglia activation is still elusive. Our results show that Ang II or PMA significantly induced NOX

activation, ROS production, and pro-inflammatory microglia activation. On the other hand, for the first time to our knowledge, we showed that AT2R via PP2A prevented PKC-induced NOX activation, ROS production, and pro-inflammatory microglia activation.

Increased ROS production by NOX activation is unswervingly related to oxidative stress that contributes to the impaired cellular functions and development of several neurodegenerative diseases [4, 10, 47]. On the other hand, NOX-2, the most predominant source for ROS in microglia, induces inflammatory activation in microglia [4, 10] during neurodegenerative diseases [48, 49]. In addition, mitochondrial dysfunction has been established as a foremost physiological disturbance in neurodegenerative diseases like AD and PD [11, 50] and NOX-mediated ROS has been associated with the mitochondrial dysfunction [14]. Similarly, we also observed that Ang II or PMA induced NOX-2 activation (increased expression of $gp91^{phox}$, $p47^{phox}$, and $p22^{phox}$), ROS generation, mitochondrial dysfunction (increased mitochondrial ROS, membrane depolarization and mitochondrial respiration), and polarization of microglia toward cytotoxic pro-inflammatory phenotype. On the contrary, stimulation of AT2R prevented NOX activation, ROS generation, mitochondrial dysfunction, and polarization of microglia toward cytotoxic pro-inflammatory phenotype in Ang II- or PMA-stimulated microglia. The inhibitory effect of AT2R was of as much magnitude as DPI (NOX inhibitor), NAC (ROS scavenger), and mito-Tempo (mitochondrial ROS inhibitor), indicating the strong anti-oxidant effect due to AT2R activation. Similarly, previous reports have demonstrated that pharmacological or genetic modulation of NOX-2 attenuated pro-inflammatory activation of microglia [4, 11] and mitochondrial dysfunction with pro-inflammatory phenotype [51, 52]. These observations strongly suggest that AT2R activation, by inhibiting NOX-induced ROS generation and mitochondrial dysfunction prevents Ang II- or PMA-induced pro-inflammatory microglia activation. Further, we identify the AT2R as a novel target for improving mitochondrial functions in microglia.

The previous studies have demonstrated that Ang II- or PMA-induced PKC activation is the pivotal mechanism of NOX activation (by phosphorylation of $p47^{phox}$) and ROS generation [12–14]. In addition, PP2A, a major serine/threonine phosphatase, is known to inactivate PKC and $p47^{phox}$ by dephosphorylation [12, 53]. Our study also revealed that stimulation of AT2R induced PP2A activation resulting in the inhibition of PKC, dephosphorylation of $p47^{phox}$, and NOX suppression in Ang II- or PMA-stimulated microglia, the effect which was promoted by PKC inhibitor, Rottlerin and reversed by PP2A inhibitor, OA. Likewise, it has previously been reported that PP2A might result in the dephosphorylation of $p47^{phox}$ [54] preventing its translocation and activation of NOX [54]. Therefore, the robust anti-oxidant effect of AT2R activation in this study might be due to the dual inhibition of NOX activation, either by dephosphorylation of $p47^{phox}$ or PKC inactivation in microglia. Importantly, we observed that p47KO microglia were immune to Ang II or PMA induced NOX activation and ROS generation indicating the pivotal role of $p47^{phox}$ in inducing Ang II or PMA mediated NOX activation and pro-inflammatory microglia activation. Therefore our results suggested that AT2R via PP2A activation results in PKC inactivation, $p47^{phox}$ dephosphorylation, attenuation of NOX-mediated ROS generation and pro-inflammatory microglia activation.

Pro-inflammatory microglia-mediated inflammation, a major contributor of neuronal injury and death, is presumably due to the production of elevated levels of cytotoxic factors and decrease in the neurotrophic levels [55, 56]. In the present study, we also observed that CM from Ang II-activated microglia induced apoptosis in the neuronal cells (Neuro-2A cells). However, CM from AT2R-activated microglia prevented the neuronal death. Similarly, earlier reports demonstrated that CM from LPS-activated microglia induced cell death in SH-SY5Y neuronal cells and loss of TH-positive cells in primary mesencephalic cultures [57]. These observations functionally confirmed the prevention of neurotoxic phenotype in Ang II-stimulated microglia by AT2R activation.

The systemic administration of LPS is associated with sickness behavior, resulting in decreased locomotor activity and pro-inflammatory microglia activation [42]. We also observed the sickness behavior in LPS-injected mice. However, AT2R activation by CGP inhibited the LPS-induced sickness behavior. Importantly, LPS-induced sickness behavior was completely prevented in p47KO mice. This indicates that AT2R activation or NOX inhibition is central to the amelioration of sickness behavior in LPS-treated mice. Similar effects were reported earlier after NOX inhibition in LPS-injected mice/rats [58]. Of note, AT2R activation or p47KO prevented the LPS-induced ROS generation, pro-inflammatory microglia activation, while promoting the immunoregulatory phenotype. The beneficial effects of AT2R activation in our study might be, at least in part, due to the polarization of microglia to anti-inflammatory phenotype and suppression of NOX activation. However, we do not exclude the CGP effects in other target cells, like neurons and brain endothelium [22, 23]. Taken together, these results strongly indicate that AT2R activation or NOX inhibition attenuates pro-inflammatory microglia activation and sickness behavior in vivo.

In conclusion, our data revealed, for the first time to our knowledge, that AT2R via PP2A activation prevented the Ang II- or PMA-induced PKC activation, phosphorylation of $p47^{phox}$ and pro-inflammatory activation of microglia, an effect that was promoted by PKC-inhibitor Rottlerin and reversed by the PP2A inhibitor, Okadaic acid. p47KO microglia were resistant/immune to Ang II- or PMA-induced NOX

activation and pro-inflammatory microglial activation. Of note, LPS treatment in p47KO mice or AT2R activation prevented ROS generation, pro-inflammatory microglial activation, and sickness behavior in vivo. Thus, we have identified AT2R as a novel therapeutic target for inflammatory brain diseases by preventing pro-inflammatory activation of microglia.

Acknowledgments We are extremely thankful to Dr. Kumaravelu Jagavelu (CSIR-CDRI) for providing the genotyped WT and KO mice used in the studies. We are highly thankful to Mr. A. L. Vishwakarma, Mrs. M. Chaturvedi, and Mr. Dhananjay Sharma for help with the flow cytometry and confocal microscopy procedures. We are highly thankful to Mr. Jitender Singh Kanshana and Mr. Anant Jaiswal for help in real-time PCR studies. We also acknowledge THUNDER (BSC0102) and MoES (GAP0118) for the confocal facility. The CSIR-CDRI communication number of this article is 9722.

Funding Information The study was supported by a financial grant to Kashif Hanif from Department of Biotechnology (DBT, Grant No. BT/PR4021/MED/30/676/2011) and CSIR Network Project MIND (BSC0115). Award of research fellowships to SAB from the Indian Council of Medical Research (ICMR), New Delhi and AS from NIPER, Rae Bareli, are greatly acknowledged.

Compliance with Ethical Standards

Conflict of Interest The authors declare that they have no conflict of interest.

References

1. Perry VH, Nicoll JA, Holmes C (2010) Microglia in neurodegenerative disease. Nat Rev Neurol 6:193–201
2. Yenari MA, Xu L, Tang XN, Qiao Y, Giffard RG (2006) Microglia potentiate damage to blood-brain barrier constituents: improvement by minocycline in vivo and in vitro. Stroke 37:1087–1093
3. Saijo K, Glass CK (2011) Microglial cell origin and phenotypes in health and disease. Nat Rev Immunol 11:775–787
4. Rojo AI, McBean G, Cindric M, Egea J, Lopez MG, Rada P, Zarkovic N, Cuadrado A (2014) Redox control of microglial function: molecular mechanisms and functional significance. Antioxid Redox Signal 21:1766–1801
5. Salemi J, Obregon DF, Cobb A, Reed S, Sadic E, Jin J, Fernandez F, Tan J et al (2011) Flipping the switches: CD40 and CD45 modulation of microglial activation states in HIV associated dementia (HAD). Mol Neurodegener 6:3
6. Hu X, Leak RK, Shi Y, Suenaga J, Gao Y, Zheng P, Chen J (2015) Microglial and macrophage polarization-new prospects for brain repair. Nat Rev Neurol 11:56–64
7. Andersen JK (2004) Oxidative stress in neurodegeneration: cause or consequence? Nat Med 10(Suppl):S18–S25
8. Mariani E, Polidori MC, Cherubini A, Mecocci P (2005) Oxidative stress in brain aging, neurodegenerative and vascular diseases: an overview. J Chromatogr B Analyt Technol Biomed Life Sci 827:65–75
9. Nakagawa Y, Chiba K (2014) Role of microglial m1/m2 polarization in relapse and remission of psychiatric disorders and diseases. Pharmaceuticals (Basel) 7:1028–1048
10. Bedard K, Krause KH (2007) The NOX family of ROS-generating NADPH oxidases: physiology and pathophysiology. Physiol Rev 87:245–313
11. Choi SH, Aid S, Kim HW, Jackson SH, Bosetti F (2012) Inhibition of NADPH oxidase promotes alternative and anti-inflammatory microglial activation during neuroinflammation. J Neurochem 120:292–301
12. Egger T, Schuligoi R, Wintersperger A, Amann R, Malle E, Sattler W (2003) Vitamin E (alpha-tocopherol) attenuates cyclo-oxygenase 2 transcription and synthesis in immortalized murine BV-2 microglia. Biochem J 370(Pt 2):459–467. https://doi.org/10.1042/BJ20021358
13. Rodriguez-Pallares J, Rey P, Parga JA, Munoz A, Guerra MJ, Labandeira-Garcia JL (2008) Brain angiotensin enhances dopaminergic cell death via microglial activation and NADPH-derived ROS. Neurobiol Dis 31:58–73
14. Rodriguez-Perez AI, Borrajo A, Rodriguez-Pallares J, Guerra MJ, Labandeira-Garcia JL (2015) Interaction between NADPH-oxidase and rho-kinase in angiotensin II-induced microglial activation. Glia 63:466–482
15. Liao B, Zhao W, Beers DR, Henkel JS, Appel SH (2012) Transformation from a neuroprotective to a neurotoxic microglial phenotype in a mouse model of ALS. Exp Neurol 237:147–152
16. Saavedra JM (2012) Angiotensin II AT(1) receptor blockers as treatments for inflammatory brain disorders. Clin Sci (Lond) 123:567–590
17. Tota S, Kamat PK, Saxena G, Hanif K, Najmi AK, Nath C (2012) Central angiotensin converting enzyme facilitates memory impairment in intracerebroventricular streptozotocin treated rats. Behav Brain Res 226:317–330
18. Grammatopoulos TN, Jones SM, Ahmadi FA, Hoover BR, Snell LD, Skoch J, Jhaveri VV, Poczobutt AM et al (2007) Angiotensin type 1 receptor antagonist losartan, reduces MPTP-induced degeneration of dopaminergic neurons in substantia nigra. Mol Neurodegener 2:1
19. Bhat SA, Goel R, Shukla R, Hanif K (2016) Angiotensin receptor blockade modulates NFκB and STAT3 signaling and inhibits glial activation and neuroinflammation better than angiotensin-converting enzyme inhibition. Mol Neurobiol 53(10):6950–6967
20. Yamamoto S, Yancey PG, Zuo Y, Ma L-J, Kaseda R, Fogo AB, Ichikawa I, Linton MF et al (2011) Macrophage polarization by angiotensin II-type 1 receptor aggravates renal injury-acceleration of atherosclerosis. Arterioscler Thromb Vasc Biol 31(12):2856–2864. https://doi.org/10.1161/ATVBAHA.111.237198
21. Dikalov SI, Nazarewicz RR (2013) Angiotensin II-induced production of mitochondrial reactive oxygen species: potential mechanisms and relevance for cardiovascular disease. Antioxid Redox Signal 19:1085–1094
22. McCarthy CA, Facey LJ, Widdop RE (2014) The protective arms of the renin-angiontensin system in stroke. Curr Hypertens Rep 16:440
23. McCarthy CA, Vinh A, Callaway JK, Widdop RE (2009) Angiotensin AT2 receptor stimulation causes neuroprotection in a conscious rat model of stroke. Stroke 40:1482–1489
24. Labandeira-Garcia JL, Rodríguez-Perez AI, Garrido-Gil P, Rodriguez-Pallares J, Lanciego JL, Guerra MJ (2017) Brain renin-angiotensin system and microglial polarization: implications for aging and neurodegeneration. Front Aging Neurosci 9:129. https://doi.org/10.3389/fnagi.2017.00129
25. Guimond MO, Gallo-Payet N (2012) How does angiotensin AT(2) receptor activation help neuronal differentiation and improve neuronal pathological situations? Front Endocrinol (Lausanne) 3:164
26. Iwai M, Liu HW, Chen R, Ide A, Okamoto S, Hata R, Sakanaka M, Shiuchi T et al (2004) Possible inhibition of focal cerebral ischemia by angiotensin II type 2 receptor stimulation. Circulation 110:843–848
27. Reinecke K, Lucius R, Reinecke A, Rickert U, Herdegen T, Unger T (2003) Angiotensin II accelerates functional recovery in the rat

sciatic nerve in vivo: role of the AT2 receptor and the transcription factor NF-kappaB. FASEB J 17:2094–2096
28. Li J, Culman J, Hortnagl H, Zhao Y, Gerova N, Timm M, Blume A, Zimmermann M et al (2005) Angiotensin AT2 receptor protects against cerebral ischemia-induced neuronal injury. FASEB J 19: 617–619
29. Li JJ, Lu J, Kaur C, Sivakumar V, Wu CY, Ling EA (2009) Expression of angiotensin II and its receptors in the normal and hypoxic amoeboid microglial cells and murine BV-2 cells. Neuroscience 158:1488–1499
30. Cooney SJ, Bermudez-Sabogal SL, Byrnes KR (2013) Cellular and temporal expression of NADPH oxidase (NOX) isotypes after brain injury. J Neuroinflammation 10:155
31. Choi J, Ifuku M, Noda M, Guilarte TR (2011) Translocator protein (18 kDa)/peripheral benzodiazepine receptor specific ligands induce microglia functions consistent with an activated state. Glia 59:219–230
32. Ye J, Jiang Z, Chen X, Liu M, Li J, Liu N (2015) Electron transport chain inhibitors induce microglia activation through enhancing mitochondrial reactive oxygen species production. Exp Cell Res 340: 315–326
33. Xie N, Li H, Wei D, LeSage G, Chen L, Wang S, Zhang Y, Chi L et al (2010) Glycogen synthase kinase-3 and p38 MAPK are required for opioid-induced microglia apoptosis. Neuropharmacology 59: 444–451
34. Wen J, Ribeiro R, Zhang Y (2011) Specific PKC isoforms regulate LPS-stimulated iNOS induction in murine microglial cells. J Neuroinflammation 8:38. https://doi.org/10.1186/1742-2094-8-38
35. Liu B, Hong JS (2003) Role of microglia in inflammation-mediated neurodegenerative diseases: mechanisms and strategies for therapeutic intervention. J Pharmacol Exp Ther 304:1–7
36. Bhat SA, Goel R, Shukla R, Hanif K (2017) Platelet CD40L induces activation of astrocytes and microglia in hypertension. Brain Behav Immun 59:173–189. https://doi.org/10.1016/j.bbi.2016.09.021
37. Maurya CK, Arha D, Rai AK, Kumar SK, Pandey J, Avisetti DR, Kalivendi SV, Klip A et al (2015) NOD2 activation induces oxidative stress contributing to mitochondrial dysfunction and insulin resistance in skeletal muscle cells. Free Radic Biol Med 89:158–169
38. Khanna V, Jain M, Singh V, Kanshana JS, Prakash P, Barthwal MK, Murthy PS, Dikshit M (2013) Cholesterol diet withdrawal leads to an initial plaque instability and subsequent regression of accelerated iliac artery atherosclerosis in rabbits. PLoS One 8:e77037
39. Maehama T, Taylor GS, Slama JT, Dixon JE (2000) A sensitive assay for phosphoinositide phosphatases. Anal Biochem 279:248–250
40. Lee JW, Lee YK, Yuk DY, Choi DY, Ban SB, Oh KW, Hong JT (2008) Neuro-inflammation induced by lipopolysaccharide causes cognitive impairment through enhancement of beta-amyloid generation. J Neuroinflammation 5:37
41. Lee S, Brait VH, Arumugam TV, Evans MA, Kim HA, Widdop RE, Jones ES (2012) Neuroprotective effect of an angiotensin receptor type 2 agonist following cerebral ischemia in vitro and in vivo. Exp Transl Stroke Med 4:16. https://doi.org/10.1186/2040-7378-4-16
42. Xi J, Lei C, Shen L, Chen Z, Xu L, Zhang J, Yu X (2016) Transastaxanthin attenuates lipopolysaccharide-induced neuroinflammation and depressive-like behavior in mice. Brain Res 1649(Pt A):30–37
43. Kinoshita D, Cohn DW, Costa-Pinto FA, de Sa-Rocha LC (2009) Behavioral effects of LPS in adult, middle-aged and aged mice. Physiol Behav 96:328–332
44. Pitychoutis PM, Nakamura K, Tsonis PA, Papadopoulou-Daifoti Z (2009) Neurochemical and behavioral alterations in an inflammatory model of depression: Sex differences exposed. Neuroscience 159:1216–1232
45. Rojo AI, Innamorato NG, Martin-Moreno AM, De Ceballos ML, Yamamoto M, Cuadrado A (2010) Nrf2 regulates microglial dynamics and neuroinflammation in experimental Parkinson's disease. Glia 58:588–598
46. Gandhi S, Abramov AY (2012) Mechanism of oxidative stress in neurodegeneration. Oxidative Med Cell Longev 2012:428010
47. Li J, Wuliji O, Li W, Jiang ZG, Ghanbari HA (2013) Oxidative stress and neurodegenerative disorders. Int J Mol Sci 14:24438–24475
48. Uttara B, Singh AV, Zamboni P, Mahajan RT (2009) Oxidative stress and neurodegenerative diseases: a review of upstream and downstream antioxidant therapeutic options. Curr Neuropharmacol 7:65–74
49. Glass CK, Saijo K, Winner B, Marchetto MC, Gage FH (2010) Mechanisms underlying inflammation in neurodegeneration. Cell 140:918–934
50. Calabrese V, Guagliano E, Sapienza M, Mancuso C, Butterfield DA, Stella AM (2006) Redox regulation of cellular stress response in neurodegenerative disorders. Ital J Biochem 55:263–282
51. Apostolova N, Blas-Garcia A, Esplugues JV (2011) Mitochondria sentencing about cellular life and death: a matter of oxidative stress. Curr Pharm Des 17:4047–4060
52. Orihuela R, McPherson CA, Harry GJ (2016) Microglial M1/M2 polarization and metabolic states. Br J Pharmacol 173:649–665
53. Kirchhefer U, Heinick A, König S, Kristensen T, Müller FU, Seidl MD, Boknik P (2014) Protein phosphatase 2A is regulated by protein kinase Cα (PKCα)-dependent phosphorylation of its targeting subunit B56α at Ser41. J Biol Chem 289(1):163–176
54. Chia KKM, Liu C-C, Hamilton EJ, Garcia A, Fry NA, Hannam W, Figtree GA, Rasmussen HH (2015) Stimulation of the cardiac myocyte Na+-K+ pump due to reversal of its constitutive oxidative inhibition. Am J Physiol Cell Physiol 309(4):C239–C250. https://doi.org/10.1152/ajpcell.00392.2014
55. Minghetti L, Levi G (1998) Microglia as effector cells in brain damage and repair: Focus on prostanoids and nitric oxide. Prog Neurobiol 54:99–125
56. Domercq M, Vazquez-Villoldo N, Matute C (2013) Neurotransmitter signaling in the pathophysiology of microglia. Front Cell Neurosci 7:49–176. https://doi.org/10.1074/jbc.M113.507996
57. Chien CH, Lee MJ, Liou HC, Liou HH, Fu WM (2016) Microglia-derived cytokines/chemokines are involved in the enhancement of LPS-induced loss of nigrostriatal dopaminergic neurons in DJ-1 knockout mice. PLoS One 11:e0151569
58. Benicky J, Sanchez-Lemus E, Honda M, Pang T, Orecna M, Wang J, Leng Y, Chuang DM et al (2011) Angiotensin II AT1 receptor blockade ameliorates brain inflammation. Neuropsychopharmacology 36: 857–870